Available online at www.sciencedirect.com
SCIENCE DIRECT®
Precambrian Research 146 (2006) 68–92
Precambrian Research
www.elsevier.com/locate/precamres

Chemostratigraphic and sedimentological framework of the largest negative carbon isotopic excursion in Earth history: The Neoproterozoic Shuram Formation (Nafun Group, Oman)

Erwan Le Guerroué [a,*], Philip A. Allen [a,1], Andrea Cozzi [a]

[a] *Geological Institute, Department of Earth Sciences, ETH-Zentrum, Sonneggstrasse, 5 8092 Zürich, Switzerland*

Received 24 August 2005; received in revised form 9 January 2006; accepted 10 January 2006

Abstract

Oman records in its Neoproterozoic Nafun Group (Huqf Supergroup) an essentially complete, carbonate-rich Ediacaran succession. The Nafun Group overlies the presumed Marinoan rift-related Fiq Member (ca. 635 Ma) and ends just below the Precambrian–Cambrian boundary (542 Ma). Tectonic subsidence caused by thermal contraction following Fiq-aged rifting allowed the preservation of about 1 km of postrift stratigraphy, with no major stratigraphic breaks. The Nafun Group above the Marinoan cap carbonate (Hadash Formation) represents two siliciclastic to carbonate 'grand cycles', both initiated by significant transgressions: these cycles comprise the Masirah Bay/Khufai formations and the Shuram/Buah formations. The Khufai–Shuram boundary is associated with the start of a major carbon isotope perturbation. The uppermost ramp carbonates of the Khufai Formation record a smooth decrease in $\delta^{13}C$ from about +4‰ to values around 0, followed by two descending steps across which values plunge to a nadir of −12‰ in the overlying red siltstones and shales interbedded with thin limestones of the Shuram Formation. This fall in isotopic values is temporally rapid and coincident in both shallow and deep-water sections in the time span of a single parasequence. The $\delta^{13}C$ nadir is then followed by 50 million years of monotonic recovery.

The 'Shuram shift' represents the largest $\delta^{13}C$ inorganic carbon negative excursion in Earth history. Although the snowball Earth theory links periods of depleted carbon isotopic ratios with periods of global glaciation, the non-glaciated context of the Shuram Formation suggests that the causal relationship between global glaciation and negative carbon isotopic excursions is non-unique. Although the precise mechanism driving this major perturbation of the carbon cycle remains enigmatic, the long-term remineralization of an isotopically depleted organic carbon reservoir in ocean water is a promising candidate.

Keywords: Neoproterozoic; Ediacaran; Carbon isotopes; Nafun Group; Shuram Formation; Oman

1. Introduction

Neoproterozoic sedimentary rocks record periods of extreme climatic oscillations, including putative snowball Earth events. However, the Ediacaran period (635–542 Ma; Hoffmann et al., 2004; Knoll et al., 2004; Condon et al., 2005) contains the largest $\delta^{13}C$ excursion in inorganic carbon of marine carbonates in Earth history, possibly lasting from ca. 600 to 550 Ma (Le Guerroué et al., 2006), a time period for

* Corresponding author. Tel.: +41 1 632 8646; fax: +41 1 632 1080/1422.
E-mail address: erwan@erdw.ethz.ch (E. Le Guerroué).
[1] Present address: Department of Earth Science and Engineering, Imperial College London, South Kensington Campus, London SW7 2AZ, United Kingdom.

0301-9268/$ – see front matter © 2006 Elsevier B.V. All rights reserved.
doi:10.1016/j.precamres.2006.01.007

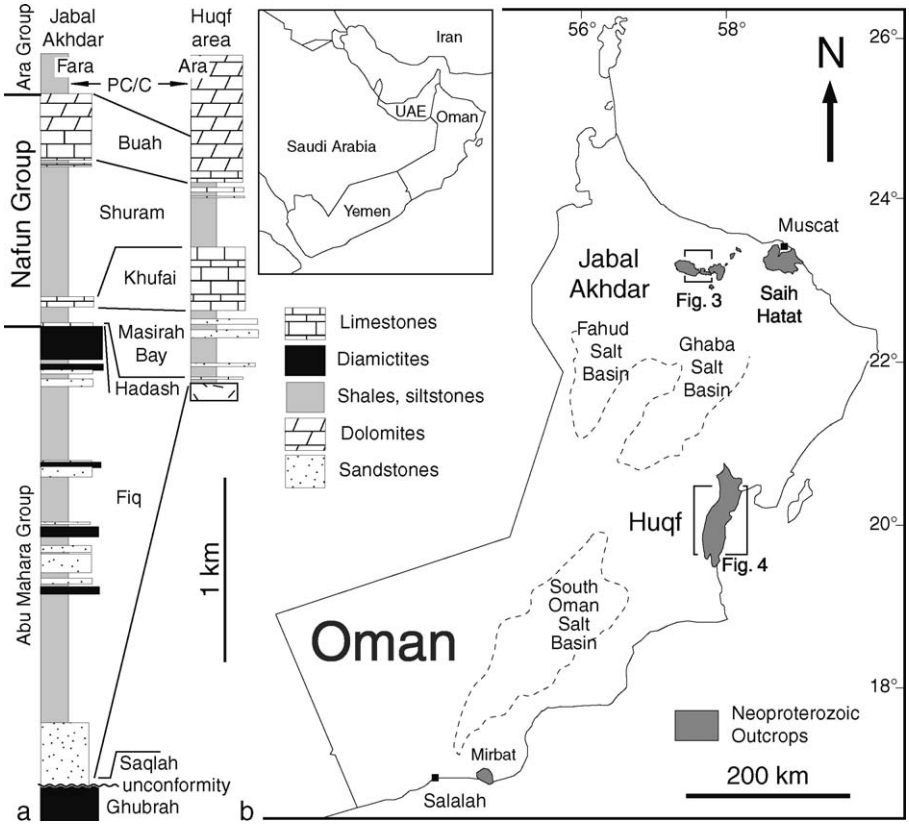

Fig. 1. (a) Simplified sedimentary logs of the Jabal Akhdar and Huqf areas. (b) Map of Oman showing Jabal Akhdar, Huqf and Mirbat regions where Neoproterozoic rocks crop out. The Saih Hatat is strongly metamorphosed and deformed and therefore excluded from the present study.

which there is no evidence for major glaciations. The Nafun Group of the Huqf Supergroup of Oman consists of a conformable >1 km-thick mixed carbonate-siliciclastic succession that appears to be unbroken by major unconformities, thereby distinguishing the Nafun Group from other less complete Ediacaran successions. The Nafun Group shows two major siliciclastic to carbonate 'grand cycles' above the Marinoan-equivalent Fiq glacial succession and its cap carbonate (Hadash Formation) (Fig. 1). The first grand cycle, composed of the Masirah Bay/Khufai formations, is associated with presumed global transgression following the Marinoan glaciation (Allen and Leather, 2006). A significant transgression also defines the base of the second Shuram/Buah grand cycle. The origin of the transgression initiating the second grand cycle remains uncertain since no glacial deposits have been shown to precede the cycle. The Gaskiers glaciation (580 Ma, Krogh et al., 1988; Bowring et al., 2003) is believed to have been localized, and significantly postdates the start of the isotopic excursion according to the chronology of Le Guerroué et al. (2006).

The post-Marinoan transgressive 'cap sequence' (Hoffman et al., 1998) is depleted in ^{13}C with values dropping to −5‰, whereas, the trangressive base of the second grand cycle records values down to −12‰ in the Shuram Formation (Burns and Matter, 1993; Le Guerroué et al., 2006). This very large negative excursion persists through up to 1 km of overlying stratigraphy, with a cross-over to positive values within the ramp carbonates of the Buah Formation. The carbon isotopic excursion is therefore in phase with relative sea level change interpreted from sedimentary facies. A similar excursion in terms of amplitude is found in the Wonoka Formation of Australia (Calver, 2000), Johnnie Formation of SW USA (Corsetti and Kaufman, 2003), Chenchinskaya, Nikolskaya and Torginskay Formations of Siberia (Melezhik et al., 2005) and Doushantuo Formation of China (Condon et al., 2005).

The presence of a carbon isotopic excursion of this amplitude and duration is difficult to explain, since Phanerozoic negative excursions are conspicuously short-lived and represent shifts of generally less than 2‰ (e.g., Hesselbo et al., 2000; Galli et al., 2005).

A number of theories have been proposed for the isotopic shifts associated with Precambrian glaciations, including the overwhelming of the atmosphere–ocean carbon reservoir with mantle-derived carbon (−5‰; Des Marais and Moore, 1984), accumulated during a long period during which silicate weathering was largely inoperative (snowball Earth theory; Hoffman et al., 1998), the upwelling of stratified, depleted ocean water during periods of deglaciation (Grotzinger and Knoll, 1995), the destabilization of methane clathrates (Kennedy et al., 2001; Jiang et al., 2003), high rates of runoff from large tropical rivers causing efficient burial of organic carbon and subsequent release of large reservoirs of seabed methane (Schrag et al., 2002), and the oxidation of dissolved organic matter in ocean water (Rothman et al., 2003). None of these mechanisms, however, have been applied to the much longer duration and greater amplitude excursion of the Nafun Group, which requires an explanation divorced from global or near-global glaciation.

The aim of this paper is to provide the sedimentological background for the remarkable changes in the carbon cycle implied by the carbon isotope ratios recovered from marine carbonates in the essentially continuous succession of the Nafun Group of Oman. The Khufai–Shuram boundary and its chemostratigraphic signature are described in deep water facies (Jabal Akhdar, north Oman), shallow water facies (Huqf area, in east-central Oman) and integrated with regional seismic and borehole data provided by Petroleum Development Oman (PDO). In this contribution, the depositional environment and sedimentary processes that were active during deposition of the Khufai–Shuram formations are reconstructed in order to better constrain oceanographic forcing mechanisms for the large Shuram negative $\delta^{13}C$ anomaly.

2. The Ediacaran succession in Oman

2.1. Stratigraphy

The Neoproterozoic Huqf Supergroup of Oman crops out mainly in north (Jabal Akhdar), east-central (Huqf) and south (Mirbat) Oman and is also penetrated by a large number of boreholes in the salt basins of the Oman interior (Fig. 1b). The Huqf Supergroup is subdivided into three groups: the Abu Mahara, Nafun and Ara Groups (Fig. 1a; Glennie et al., 1974; Gorin et al., 1982; Hughes-Clarke, 1988; Rabu, 1988; Loosveld et al., 1996; Leather, 2001; Cozzi and Al-Siyabi, 2004; Le Guerroué et al., 2005; Allen and Leather, 2006).In the Jabal Akhdar, the Abu Mahara Group contains two distinct glacigenic intervals in the Ghubrah Formation and Fiq Member of the Ghadir Manqil Formation (Brasier et al., 2000; Leather et al., 2002; Allen et al., 2004), separated by an angular unconformity and by the basaltic volcanics and volcaniclastics of the Saqlah Formation (Fig. 1a; Le Guerroué et al., 2005). These two intervals correlate with two clusters of glacial events labelled Sturtian (700+ Ma) and Marinoan (older than 635 Ma; Condon et al., 2005), respectively (Brasier et al., 2000; Leather et al., 2002; Allen et al., 2004; Halverson et al., 2005; Le Guerroué et al., 2005). In the Huqf region, the Abu Mahara Group is absent and the Nafun Group rests directly on the felsic volcanics and volcaniclastics of the Halfayn Formation and its granodioritic basement (Platel et al., 1992; Leather, 2001; Allen and Leather, 2006).

The Nafun Group crops out in both the Jabal Akhdar and the Huqf areas. At its base is the Marinoan trangressive cap carbonate of the Hadash Formation (Leather, 2001; Allen et al., 2004; Cozzi and Al-Siyabi, 2004; Allen and Leather, 2006), which directly overlies the Fiq Member (Allen et al., 2004) of the Ghadir Manqil Formation. The Hadash Formation is overlain by two siliciclastic-carbonate depositional cycles of the Masirah Bay–Khufai formations and Shuram–Buah formations (Figs. 1 and 2Figs. 1a and 2). The Nafun Group passes upward into the carbonate-evaporite cycles of the Ara Group, defined in PDO subsurface penetrations in the Oman salt basins (Hughes-Clarke, 1988). Outcrop equivalents of the Ara Group are found in the Huqf area (Fig. 1a; Nicholas and Brasier, 2000) and in the Jabal Akhdar, where the Buah Formation is overlain by the volcaniclastics and cherty limestones of the Fara Formation (Brasier et al., 2000).

2.2. Geochronology

Both upper and lower limits of the Huqf Supergroup are calibrated by radiometric dates. An ignimbrite in the middle of the Fara Formation (Ara Group) in the Jabal Akhdar yielded a U–Pb age of 544.5 ± 3.3 Ma (Brasier et al., 2000). Recently, core material from the middle part (units A3 and A4) of the Ara Group in the South Oman Salt Basin yielded an age of 542.0 ± 0.3 Ma, representing the Precambrian–Cambrian boundary (Amthor et al., 2003), which is in good agreement with the Fara Formation age. Therefore, a reasonable estimate for the age of the top of the Nafun Group is ca. 550 Ma.

The base of the Huqf Supergroup must be older than the age of the tuffaceous ash interbedded with diamictites in the Ghubrah Formation in the Jabal Akhdar (723 + 16/−10 Ma; Brasier et al., 2000). The presence

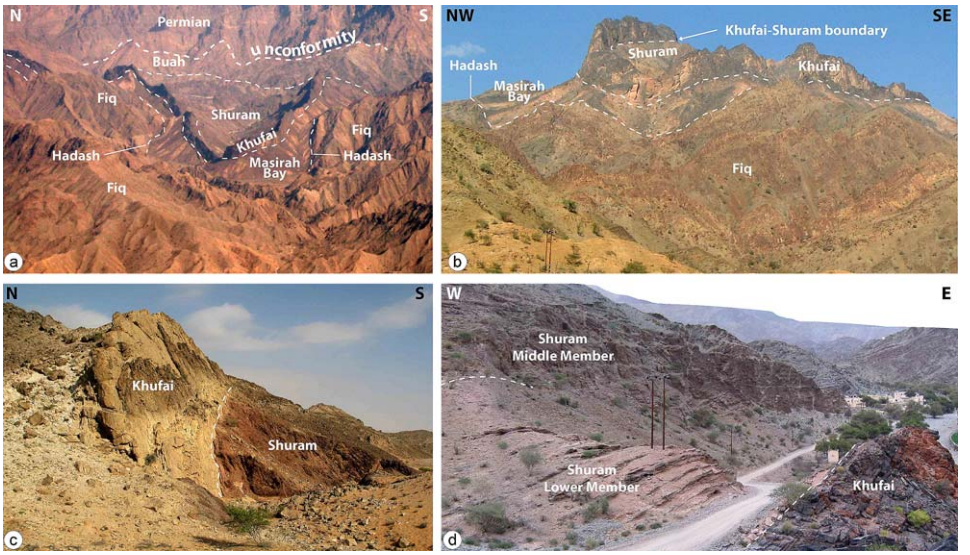

Fig. 2. Field panoramas of (a) Wadi Bani Awf anticline in the Jabal Akhdar, with Neoproterozoic stratigraphy truncated by the sub-Permian unconformity. Syncline width approximately 3 km. (b) Fiq glacigenic and non-glacial sedimentary rocks overlain by the lower part of the Nafun Group, with Shuram Formation in the core of an asymmetrical syncline, Wadi Sahtan, Jabal Akhdar. Masirah Bay is about 250 m thick. (c) Khufai–Shuram boundary in the Huqf area, showing steeply inclined Khufai Formation, a carbonate-rich upper cycle of the Khufai Formation, and a shale-dominated Shuram Formation, Mukhaibah Dome. (d) Top Khufai Formation dolomitized limestones pass up into bleached siltstones of Shuram Lower Member and then monotonous purple siltstones of the Shuram Middle Member at locality 12, Jabal Akhdar. Telegraph poles are about 5 m high.

of an angular unconformity separating the Ghubrah Formation from the Fiq Member suggests that the latter may be Marinoan in age (ending at 635 Ma; Allen et al., 2004; Condon et al., 2005; Le Guerroué et al., 2005; Bowring et al., in preparation). Therefore, the base of the Nafun Group, should this interpretation hold, is regarded to be at around 635 Ma.

3. The Nafun Group

The Nafun Group has previously been studied by Gorin et al. (1982), Wright et al. (1990) and McCarron (2000). The Hadash Formation cap carbonate and the siliciclastics of the Masirah Bay Formation strongly overstep basement margins during a major post-

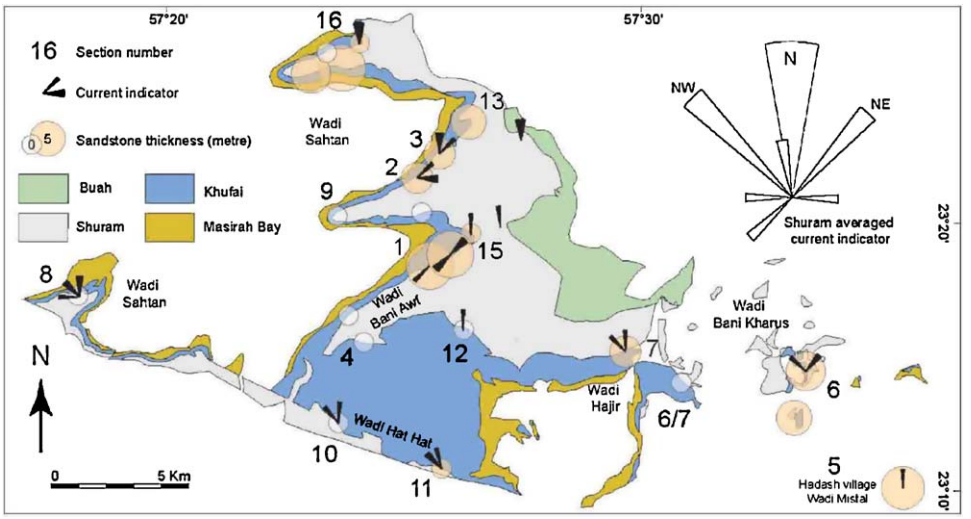

Fig. 3. Detailed geological map of the central part of the Jabal Akhdar between Wadi Bani Kharus and the eastern end of Wadi Sahtan, showing location of logged sections, with paleocurrent indicators. Thickness of the sandstone facies at top Khufai Formation is also indicated. Geological map after Rabu (1988) and Beurrier et al. (1986).

Marinoan relative sea-level rise (Allen et al., 2004; Allen and Leather, 2006). The Masirah Bay Formation then passes up gradationally into the prograding carbonate ramp of the Khufai Formation. The Masirah Bay and Khufai formations thus form the first grand cycle of the Nafun Group, sharply transgressive at its base. The overlying Shuram Formation records a significant deepening event, with deposition of siltstones and shales that pass up gradationally into the carbonate ramp of the Buah Formation. The Shuram and Buah formations therefore represent the second grand cycle of the Nafun Group, again with a transgressive base.

Although there are no radiometric dates giving depositional ages within the Nafun Group, a subsidence analysis combined with the ages of detrital zircon populations led Le Guerroué et al. (2006) to propose that the first grand cycle lasted from ca. 635 to 600 Ma and the second grand cycle from ca. 600 to 542 Ma.

3.1. The Khufai–Shuram boundary in Oman

3.1.1. Previous work

The Khufai Formation, formerly called the Hajir Formation, was described first by Kapp and Llewellyn (1965), who defined the type section in Wadi Hajir in the Oman mountains (Fig. 3). In the Huqf area, the Khufai Formation was first described by Kassler (1965) in the Khufai Dome area (KD; Fig. 4). The Khufai Formation attains a thickness of 30–100 m in the Jabal Akhdar and 250–350 m in the Huqf area, and lies conformably on top of the siliciclastic Masirah Bay Formation (Fig. 1a). Subsequent studies (Gorin et al., 1982; Wright et al., 1990; McCarron, 2000) interpreted the Khufai Formation as a carbonate ramp that passed from inner ramp peritidal facies in the Huqf area to outer ramp organic-rich limestones in the Jabal Akhdar. Khufai carbonate ramps were nucleated on basement highs and passed into deeper water conditions in intervening depressions (see below).

The Shuram Formation, formerly called the Mu'aydin Formation, was described by Kapp and Llewellyn (1965), who defined a stratotype in Wadi Mu'aydin on the south side of the Jabal Akhdar and at Wadi Shuram in the Huqf area (Kassler, 1965; WS; Fig. 4). The Shuram Formation is more than 250 m thick in the Huqf area, whereas, in the Jabal Akhdar it is approximately 700 m thick, though the thickness is not easily measured due to small and large scale folding. Subsequent studies (Gorin et al., 1982; Wright et al., 1990; McCarron, 2000) interpreted the Shuram Formation as deposited on a storm-dominated siliciclastic shelf in the Huqf area, becoming more distal towards the Jabal Akhdar.

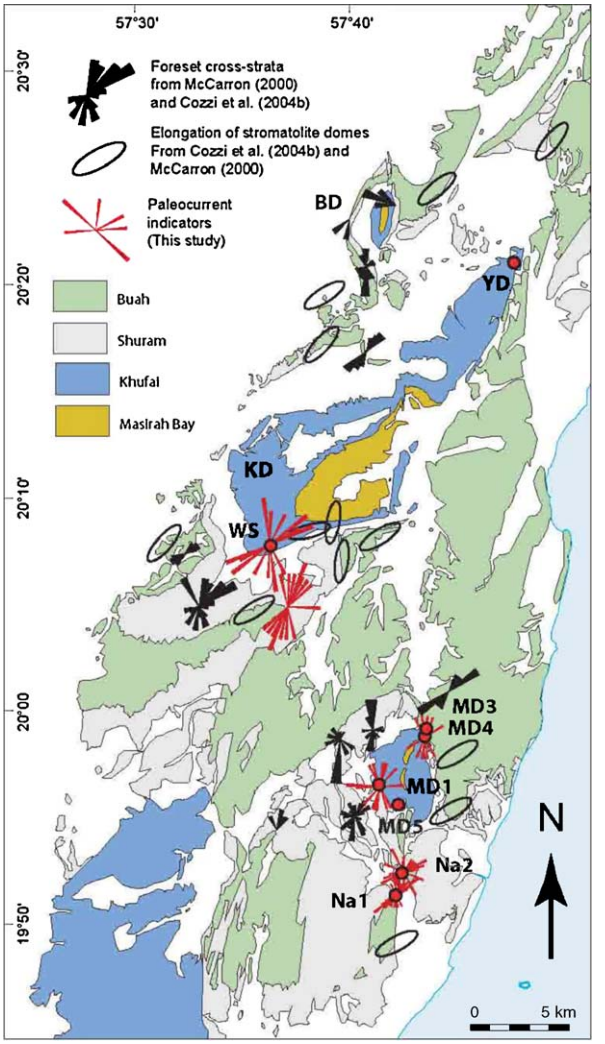

Fig. 4. Detailed geological map of the Huqf area showing section locations with paleocurrent indicators. Na1 and Na2: Nafun; BD: Buah Dome; MD1–5: Mukhaibah Dome; KD: Khufai Dome; WS: Wadi Shuram, YD: Yidah. Geological map after Dubreuilh et al. (1992) and Platel et al. (1992).

3.2. Sedimentary facies

3.2.1. Khufai formation

The Khufai Formation comprises four facies associations (A–D; Fig. 5) distributed along a homoclinal ramp (Fig. 6 and Table 1) and passes up gradationally, but over a short stratigraphic interval, into the Shuram Formation.

3.2.2. Facies association A: fetid carbonates

In the Huqf area facies association A1 consists of dark, fetid dolostones with faint centimetric planar to

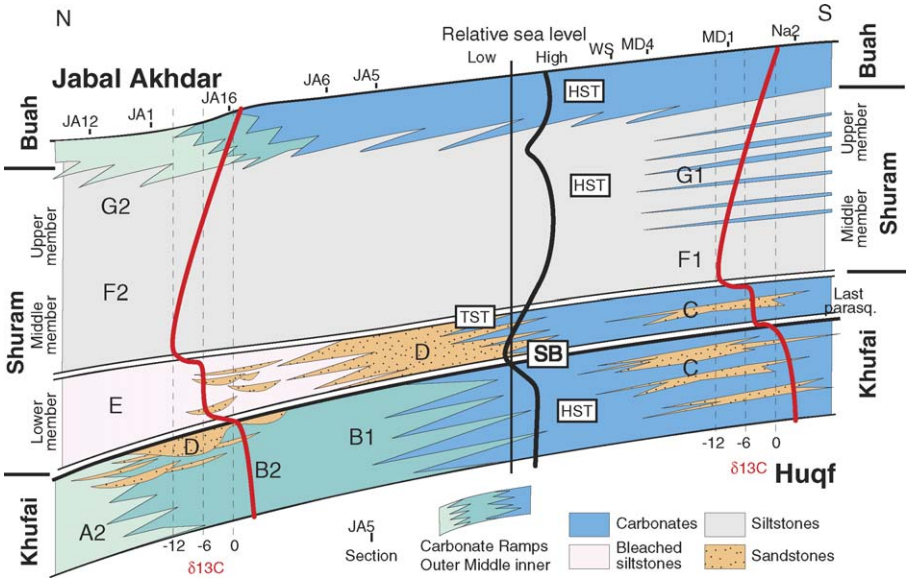

Fig. 5. Sequence stratigraphic conceptual model for the top Khufai and Shuram Formations, illustrating lateral variations between the Jabal Akhdar and Huqf area outcrops. Correlation between localities is supported by identical carbon isotopic profiles (heavy lines) between the two areas.

undulating laminations, rare evidence for cross-stratal truncations, cm-thick graded beds and cm- to m-scale slump structures with vergence generally to the northwest. In the Jabal Akhdar facies association A2 is made of black, fetid, pyritic limestone forming planar, structureless beds. Rare mudstone interbeds have commonly undergone soft sediment deformation (Table 1 and Fig. 5; McCarron, 2000).

The presence of pyrite, dark grey colouration and preservation of organic matter suggest deposition in a suboxic environment. The Huqf area sediments are considered to have been deposited in a gently sloping outer ramp setting, whereas, the Jabal Akhdar limestones

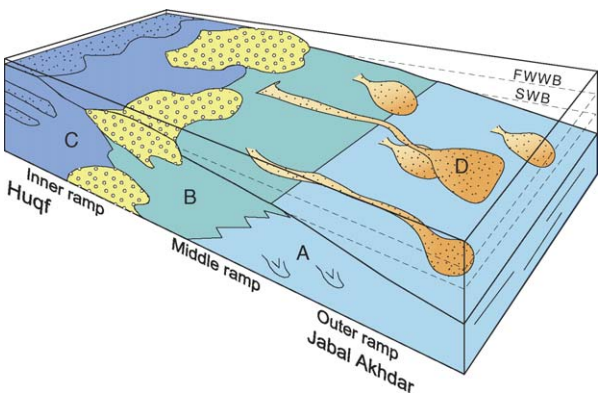

Fig. 6. Schematic block diagram showing top Khufai Formation facies distribution along a homoclinal carbonate ramp. A–D refer to facies associations described in text.

are more typical of distal outer ramp facies (Fig. 5; McCarron, 2000).

3.2.3. *Facies association B: ooidal–peloidal grainstones and stromatolites*

Facies association B (Figs. 5 and 6) is composed of grainstones with a strong facies change from east-central to north Oman. Cross-stratified ooidal/oncolitic grainstones pass into fetid, intraclastic wackestones in the northern part of the Huqf area (facies association B1; Khufai Dome and especially at Buah Dome), and then to reworked intraclast beds alternating with the fetid carbonates of facies association A1 in the mountains of north Oman (facies association B2). Cm- to m-scale stromatolites (Mukhaibah Dome) are common in the Huqf sections (Table 1; McCarron, 2000), but totally absent in those of the Jabal Akhdar.

The presence of stromatolites and associated sedimentary facies in the Huqf area indicates a well-oxygenated, moderate energy environment, possibly in a back-shoal inner ramp setting. The Khufai Dome area represents a moderate to high-energy environment in a less protected inner ramp position. The intraclastic/peloidal wackestones of the Buah Dome indicate deposition below fair weather wave base, probably in a storm-dominated mid ramp setting. The Jabal Akhdar reworked intraclast beds and fetid carbonates are more typical of slope ramp facies. Such a lateral variation represents facies changes across a north-deepening ramp (Fig. 6; McCarron, 2000).

Table 1
Facies associations of Khufai and Shuram Formations in the Jabal Akhdar and Huqf areas

Facies association		Sedimentary structures	Interpretation
Huqf area			
Khufai			
A1	Black fetid dolostones	Centimetric planar to undulating laminations, rare cross-stratal truncations, cm-thick graded beds and cm–m scale slumps	Gently sloping anoxic–suboxic outer ramp
B1	Grainstones passing into fetid, intraclastic wackestones	Scours, swaley and cross-stratification, soft sediment deformation, stromatolites	Storm dominated shallow mid ramp
Ca	Ooidal/peloidal grainstones with rounded and flattened intraclasts	Cross-stratified beds with grainstone and stromatolite clasts	Subtidal, high energy
Cb	Mudstones with mm-scale siltstone and sandstone beds	Structureless	Protected shallow subtidal, probably lagoon margins
Cc	Microbially laminated packstones, chertified evaporite cm-thick lenses	Planar, box-like and conical stromatolites, trochoidal wave ripples	Shallow subtidal (lagoonal), inner ramp
Cd	Sandstones, siltstones	Mini-ripples and bidirectional cross-strata	Wave- and tide-influenced shallow subtidal, inner ramp
Shuram			
F1	Siltstones with rare calcareous silty interbeds	Small wave ripples, sets of swaley cross-stratification and rare planar beds	Storm influenced shelf
G1	Siltstones and ooidal grainstones containing intraclasts	Soft sediment deformation, climbing wave ripples, swaley cross-stratification, planar beds and edge wise conglomerates, in progressively thickening parasequences	Stormy proximal shelf to shoreface
Jabal Akhdar			
Khufai			
A2	Black, fetid, pyritic limestone and rare mudstone interbeds	Planar lamination, structureless beds, soft sediment deformation	Distal outer ramp
B2	Intraclast grainstones alternating with facies association A	Scours, swaley and cross-stratification, soft sediment deformation	Shallow mid ramp
Da	Siltstones dispersed in facies association B	Unidirectional current ripples, graded and slumped beds	Storm influenced outer shelf
Db	Sandstone channels with cm-long intraclasts of reworked mudstones and siltstones, ooids	Rare unidirectional cross-strata, oscillatory and combined flow ripples	Lower shoreface to inner shelf
Shuram			
E	M-thick dolomitized mudstones alternating with bleached siltstones	Convolute bedding, cm–m scale slump structures, organic-rich	Outer shelf
F2	Monotonous shales with local silty carbonate beds	Unidirectional current ripples, rare climbing wave ripples and hummocky cross-stratification	Lower shoreface to inner shelf
G2	Shale and mudstone interbeds	Rare edgewise conglomerates, m-scale asymmetric-symmetric parasequences	Inner shelf

3.2.4. Facies association C: peritidal shallowing-upward m-scale cycles

Facies association C is restricted to outcrops in the Huqf area. At the same stratigraphic position, the Jabal Akhdar sections contain facies association B2 and A2, eventually passing up vertically into D (Table 1 and Figs. 5 and 6). The cycles of facies association C in the upper Khufai Formation mark the demise of the carbonate ramp in the Huqf area.

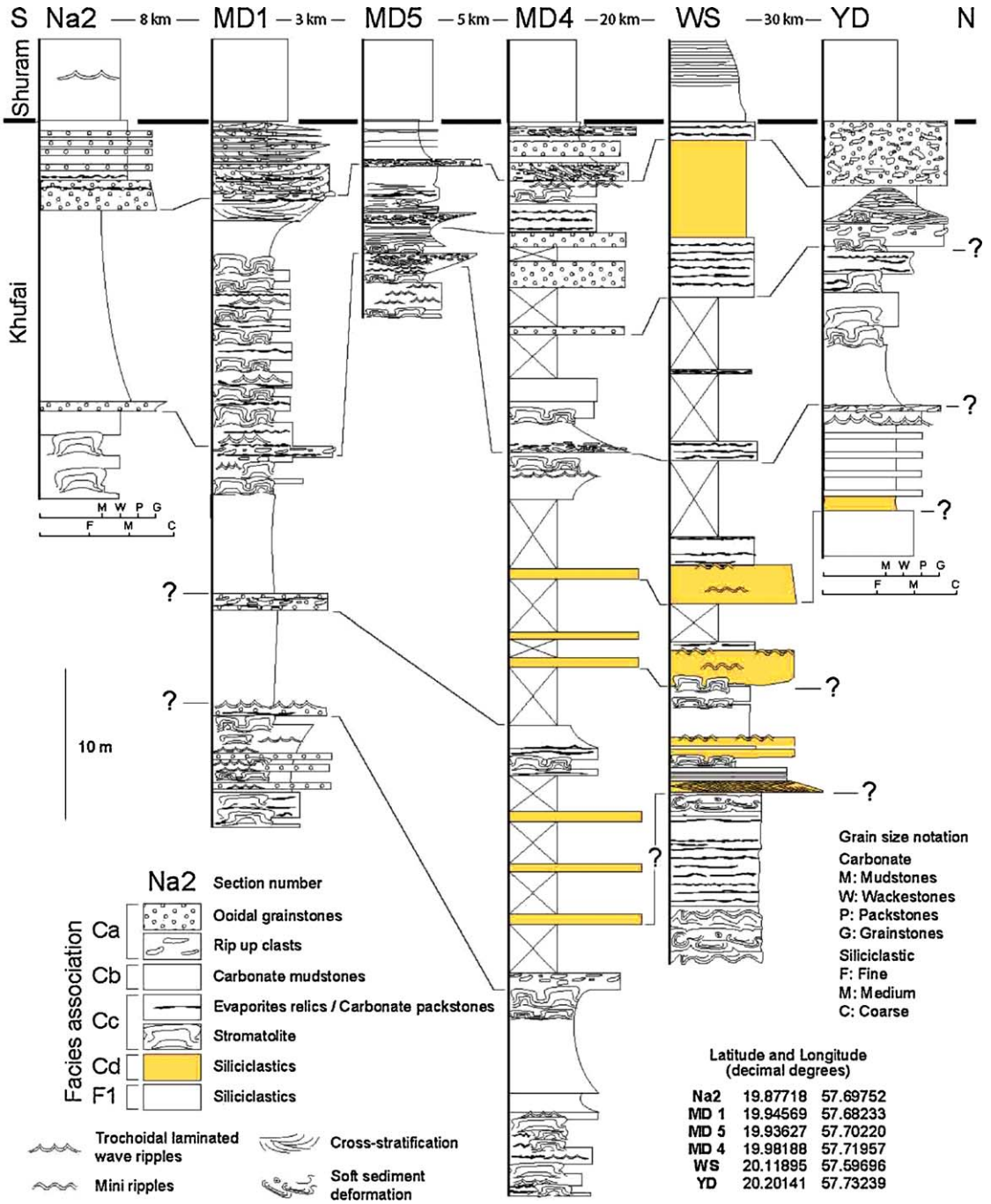

Fig. 7. Detailed sedimentary logs of the top Khufai Formation cycles in the Huqf area. Note that the Khufai–Shuram boundary is placed after the last carbonate-dominated cycle or parasequence. The last carbonate-rich parasequence is equivalent in age to the Lower Member of the Shuram Formation in the Jabal Akhdar.

Fig. 8. Field panorama of top Khufai Formation in the Huqf area at locality WS. Note the shallowing upward cycles shown by arrows. Bushes are about 1.5 m tall.

Facies association C is dominated by m-scale cycles (2–5 m) recognized by recessive bases and resistant cherty caps (Figs. 7 and 8). The cycles comprise, from base to top, ooidal/peloidal grainstones containing large (few dm), rounded and flattened intraclasts (Ca; Figs. 7 and 9c), cross-stratified beds and channel-fills (YD section) with grainstone and stromatolite clasts. The cycles are capped by mudstones with mm-scale siltstone and sandstone beds (Cb) passing up into planar, box-like and conical stromatolites (facies Cc, Figs. 7 and 9d), and locally (Mukhaibah Dome) trochoidal wave rippled packstones. Wave ripples have spacings between 5 and 11 cm and steepnesses (vertical form index) of 5–6.7, indicating that they are vortex ripples (Cc, Figs. 7 and 9g). Facies Cc also contains abundant chertified cm-thick lenses (Figs. 7 and 9b), probably resulting from chertification of lozenge-shaped evaporite mineral precursors. Wright et al. (1990) describe anhydrite inclusions in lutecite rosettes with possibly anhydrite as the precursor mineral.

The m-scale cycles are rare in the Buah Dome, where a calcareous quartz arenite is found (McCarron, 2000). Wright et al. (1990) report dolomite flake breccias in siltstone channels in this facies. This siliciclastic facies (Cd) interfingers with facies association Ca and Cb in the Khufai Dome (WS), the YD section and north Mukhaibah Dome (MD4), where medium siltstones to coarse sandstones in m-scale beds contain mini-ripples and bidirectional cross-strata (Figs. 7 and 9e, f).

Facies Ca was deposited in subtidal, high-energy environments, locally as tidal bars (YD section). The structureless mudstones and wackestones of facies Cb represent deposition in protected shallow subtidal environments, probably in lagoon margins with a minor detrital supply. Cc represents evaporitic shallow subtidal-stromatolitic intertidal (lagoonal) environments. Siliciclastic facies Cd requires some continental (possibly aeolian) input, probably from the Buah dome area, where the most siliciclastic sand at this interval occurs.

The presence of bimodal, herringbone cross-stratification demonstrates the influence of tides, and the mini-ripples are interpreted as due to wave action in extremely shallow water depths, which together suggest shallow subtidal to intertidal depositional environments. Analysis of the trochoidal wave ripples found near the top of the Khufai Formation in the Mukhaibah Dome area using the method of Allen (1981, 1984), recently applied to very large ripple structures in Marinoan cap carbonates (Allen and Hoffman, 2005), indicates that maximum periods of formative waves were small (ca. 2 s), suggesting locally generated waves acting in shallow water, most likely in a protected inner ramp setting.

All sections show a repeated stack of subtidal facies (Ca) and shallow subtidal facies (Cb/Cc). Base and top facies transitions of each cycle are sharp in most cases, but the transition from grainstones (Ca) to evaporite-bearing mudstones (Cb/Cc) is gradual. Consequently, these m-scale cycles are interpreted as small shallowing upward parasequences (Figs. 7 and 8).

Although facies association C reflects very shallow water depths at the top of the ramp sequence, no evidence for subaerial exposure in the form of major erosion surfaces, paleosols or karstification has been identified.

3.2.5. *Facies association D: intermixed siltstones and sandstones*

Facies association D is only found in the Jabal Akhdar on top of facies association B (Fig. 5). It records input of siliciclastics at the top of the Khufai carbonate ramp. Siliciclastics occur as dispersed quartz grains in a carbonate matrix (forming discontinuous cm-thick layers or graded in the carbonates; Da), whereas, at a stratigraphically higher level, coarser clastics (Db) are found in erosive channel-fills eroded into facies association B and the thinly bedded pinkish mudstones of facies association E (see below; Table 1). Facies association D marks the demise of the carbonate ramp in the Jabal Akhdar.

Facies association Da comprises siltstones intercalated in the carbonates of facies association B as cm-thick layers, and as graded basal layers of carbonate beds. They show unidirectional current ripples, shallow erosive and slumped beds (Fig. 10f). Regional paleocurrent indicators show a roughly northward-directed flow at the time of deposition (Fig. 3).

Coarser clastics form shallow, erosive, m-thick channels, with abundant flattened cm-size clasts of reworked pink mudstones and siltstones, ooids and carbonate

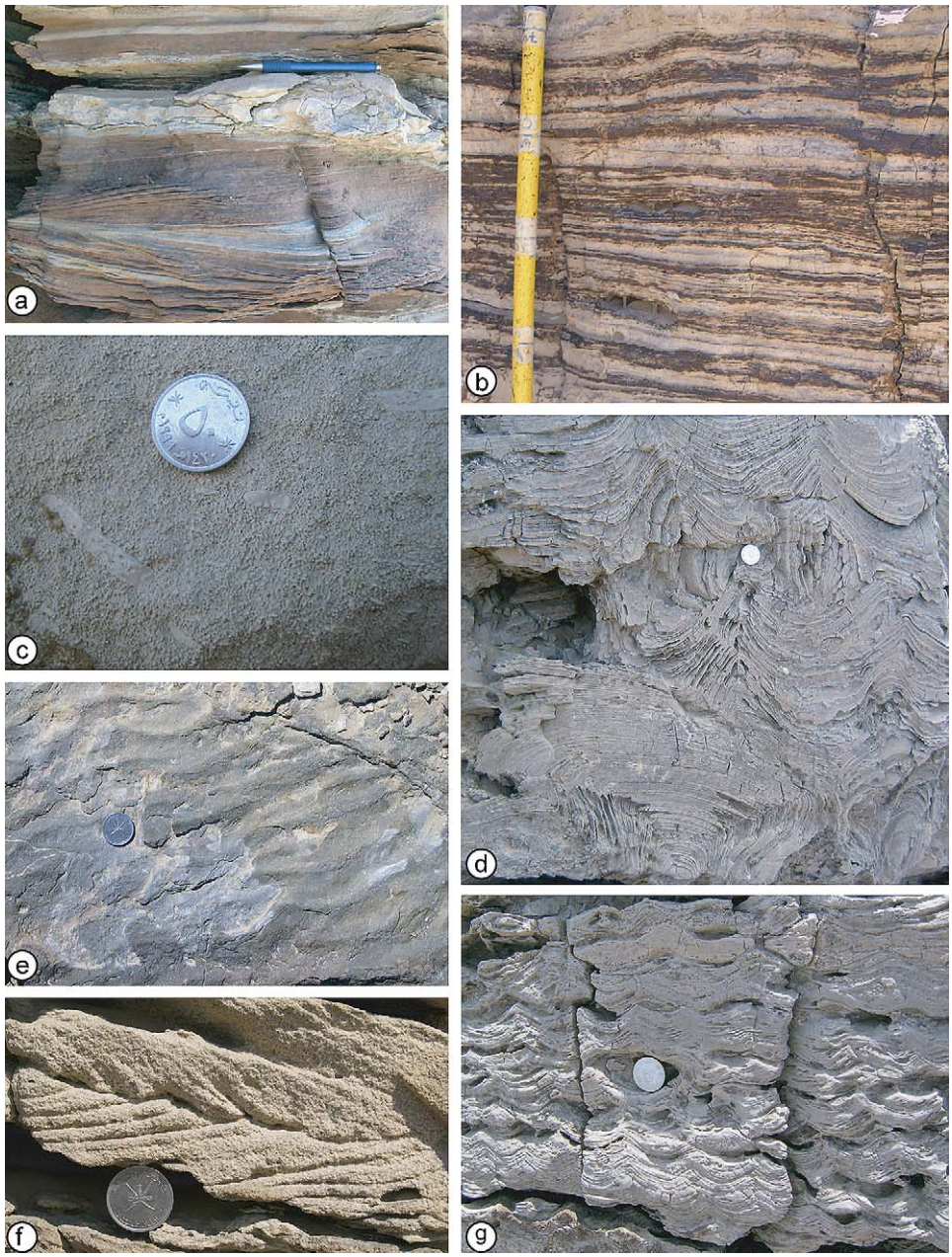

Fig. 9. Facies typical of the Huqf area. (a) Swaley cross-stratified siltstones and intraclast ooidal grainstones (below pencil) of facies association F1 at location WS. Pencil is 18 cm; (b) chertified wackestones with evaporite relics of facies association Cc at location WS. Image is 40 cm high; (c) intraclast ooidal grainstones of facies association Ca at location YD; (d) box-like stromatolite (bottom of picture) and conophytons (near coin) of facies association Cc at location MD4; (e) planform view of wave-rippled sandstone of facies association Cd at location WS; (f) tidal bidirectional (herring-bone) cross-stratified sandstones of facies association Cd at locality WS; (g) trochoidally wave-rippled wackestones of facies association Cc at locality MD5. Coin is 2.5 cm in width.

intraclasts (facies Db; Fig. 10e). Sandstone channels contain rare unidirectional cross-strata (Fig. 10c). Laterally, the channel-fills comprise clast-supported conglomerates (Section 16, for example) with dm-long, subangular, flattened intraclasts. A maximum of five channels occur at locality 1, and extend for hundreds of metres laterally, before wedging out (Figs. 3 and 11).

Some sandstone beds are dm-thick, and form laterally extensive sheets (in Section 5 in particular). The tops of beds contain dm-high symmetrical and asymmetrical

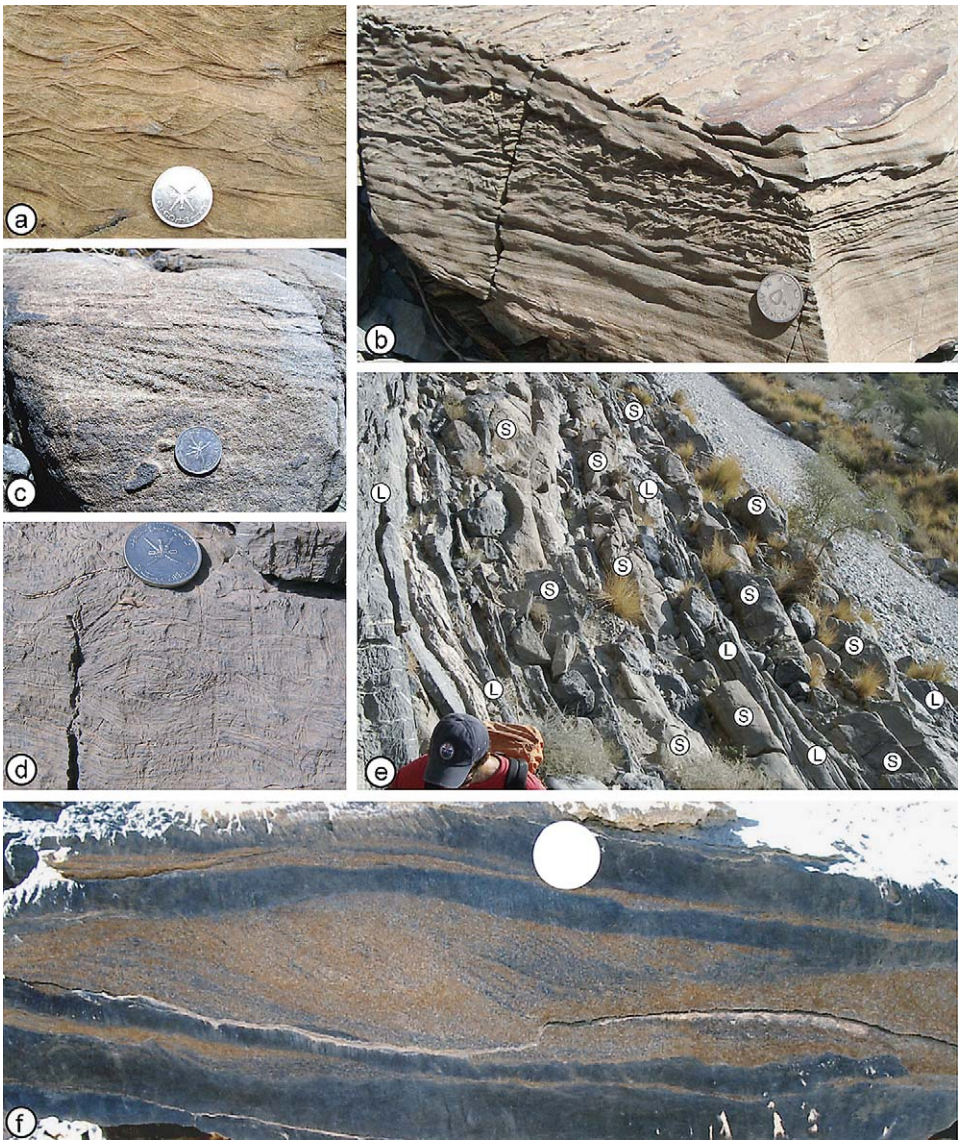

Fig. 10. Facies typical of the Jabal Akhdar area. (a) Interwoven ripple cross-lamination in grainstone of facies association F2 at location 8; (b) ripple-laminated and low-angle planar-laminated grainstones, with symmetrically rippled top surface; facies association F2 at location 1; (c) planar, unidirectional cross-stratified sandstone of facies association Db at location 1; (d) convolute micro-slumped mudstone of facies association E at locality 12; (e) Khufai–Shuram boundary region in the Jabal Akhdar; brown sandstone-filled channels (S) intercalated with mudstones and limestones (L) of facies association Db at location 1; (f) unidirectional cross-laminated form-set made of siliciclastic sandstone and grey carbonate mudstone, within the top Khufai Formation of facies association Da at location 4. Coin is about 2.5 cm width.

ripple marks with unidirectional internal foresets. Ripple wavelengths reach up to 75 cm, but more commonly are 40 cm, with heights of ∼15 cm and grain size around 0.25 mm. In plan view, they form individual hummocks or less regular three-dimensional structures. Top profiles of ripple form-sets are typically trochoidal, with thicker drapes of light grey carbonate mud in ripple troughs. Ripple profiles are slightly asymmetrical; the final stage of ripple migration is commonly recognized by a fine interlamination of quartzose sand-silt and carbonate silt, demonstrating that fine carbonate sediment was carried in suspension by the same currents that transported the coarser siliciclastic sand as bedload. Some ripple profiles appear to be modified by tectonic deformation.

The top of the Khufai carbonate ramp in the Jabal Akhdar records the deposition of the siliciclastics of facies association D (Fig. 11), which is interpreted as having been deposited mostly below storm wave base

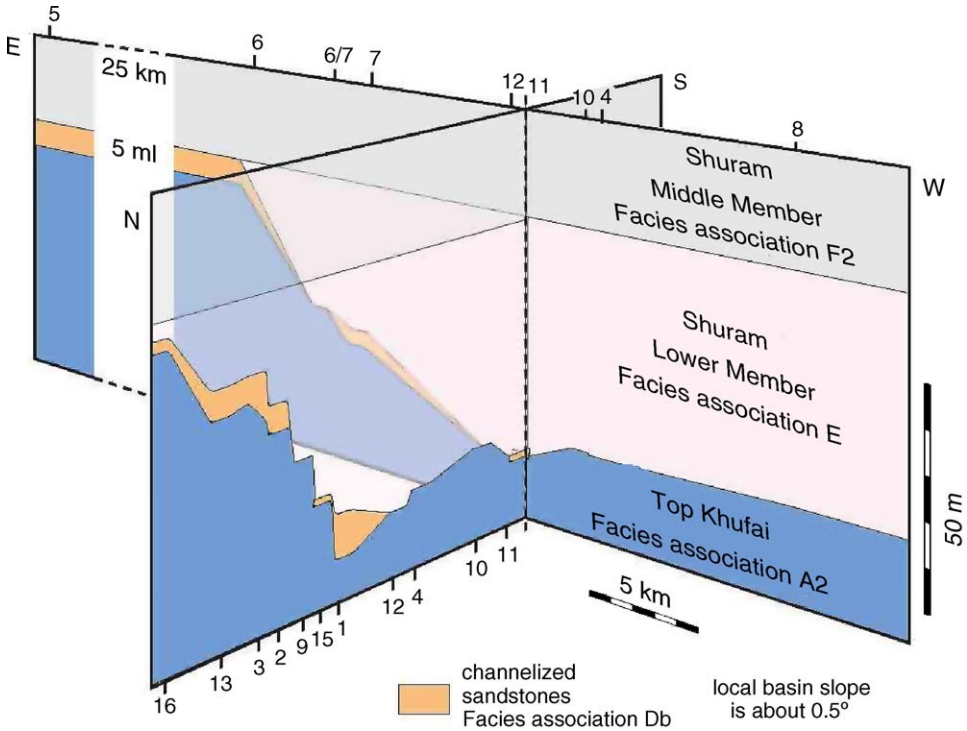

Fig. 11. Three-dimensional perspective of the geometry of the top Khufai surface and the position of channelized sandstones, using N–S and E–W profiles in the Jabal Akhdar. Note that the steepest local slopes in the basin are ca. 0.5°. Numbers at top and bottom of panels are section locations shown in Fig. 3.

(SWB). As in the Huqf area, there was most likely a shallowing of depositional environments at the top of the Khufai carbonate ramp in the Jabal Akhdar region, indicated by these siliciclastic inputs, locally (as in Section 5) reworked by oscillatory and/or combined flows (Dumas et al., 2005). Analysis of the wave ripple structures (method in Allen, 1981, 1984) indicates that maximum wave periods were up to 10 s, suggesting that the Shuram basin was large enough to allow the generation of long period waves. Shallowing of depositional environments relative to the underlying Khufai ramp is also suggested by the derivation of ooids from a shallow ramp setting. However, this shallowing of the ramp was of limited magnitude, as no major erosion surfaces or lowstand deposits have been identified. Indeed, facies association D passes to facies association E gradationally in localities where sandstones and conglomerate channels do not truncate the uppermost carbonate beds. We associate the minor relative sea level fall causing siliciclastic input and channelling with the end of the Khufai highstand.

3.3. Shuram Formation

The Shuram Formation in this study is divided into three facies associations (E–G; Fig. 5 and Table 1), corresponding to the three members of the Shuram Formation. The boundaries of the Khufai and Shuram formations are defined lithostratigraphically. However, laterally, facies association E of the Shuram Formation in the Jabal Akhdar passes to time equivalent facies association C of the Khufai Formation in the Huqf area (Fig. 5). That is, the youngest carbonate-dominated cycle (1–5 m-thick) of the Huqf area is equivalent in time to the oldest siliciclastics in the Jabal Akhdar (see chemostratigraphic section below).

3.3.1. Facies association E: dolomitic mudstones and bleached siltstones

Facies association E is found only in the Jabal Akhdar, and is made of finely convoluted m-thick dolomitized mudstones (Fig. 10e) alternating with multicoloured and bleached siltstones. Slump structures are common at the cm- to m-scale within the mudstone beds and locally involve the whole bed. Organic matter is present within the dolomitized mudstones (up to 4.5% TOC) in the form of thinly laminated black shale interbeds. Facies association E varies in thickness in the Jabal Akhdar area and thickens to 50 m towards the northwest (Fig. 11). Rarely, facies association E records minor coarser siliciclastics in the form of cm-thick siltstone and sandstone beds.

Sections 5, 6 and 16 contain only a few bleached siltstones of facies association E interbedded with the coarse channelized clastics of facies association D (Fig. 11).

The upward change into the fine-grained lithologies of facies association E, and the absence of any storm-generated features, suggests increasing water depths. Transgression is also supported by the presence of interlaminations of organic-rich black shales at the base of the facies association. The convolutions and slumps in thin mudstone beds are the result of soft sediment deformation due to shaking or gravitational instability.

Facies association E makes up the lower member of the Shuram Formation. Chemostratigraphic correlation (see Figs. 5 and 11 and below for further chemostratigraphic details) shows this facies association to correlate laterally with facies association D, which contains oscillatory and combined flow ripples. This suggests the existence of a gentle topography in the Jabal Akhdar during the time period of the Lower Member, as supported by the regional distribution of facies association E (Fig. 11). The upward transition of carbonate-dominated sediments into the siliciclastic-dominated facies association E indicates a shut-down of the Khufai carbonate factory, possibly related to climate change and/or hydrochemical changes.

3.3.2. *Facies association F: monotonous siltstones and shales*

The sediments of facies association E pass up into purple, monotonous siltstones and shales characteristic of the Shuram Formation Middle Member. The Huqf region contains siltstones with rare calcareous silty interbeds. The siliciclastics locally contain small wave ripples, sets of swaley cross-stratification and rare planar beds (F1; Table 1). The Jabal Akhdar records monotonous shales that commonly contain mm-scale, unidirectional current ripples in silty carbonate beds (F2; Table 1). Locally (Sections 1, 2 and 16), the Jabal Akhdar sections contain brownish dm-thick carbonates with climbing ripples with steep foresets (Section 4). Ripples ranging from 5 to 25 cm in wavelength and 10 cm in amplitude have their tops reworked into symmetrical profiles, but rare plan views show linguoidal ripple crestlines. These brown carbonate beds also contain detrital silt-sized quartz grains, rare wave ripples and an undulatory lamination reminiscent of hummocky cross-stratification. On the south west of the Jabal Akhdar, Section 8 shows cosets of interwoven wave ripple cross-lamination (Fig. 10a).

Rippled silty carbonate beds in the Jabal Akhdar are interpreted as having been reworked from the shallow part of the shelf and resedimented during storms under oscillatory and combined flow. However, they are rare and their distribution is probably linked to local basin highs. Storm influence is also evident in the Huqf region. Monotonous siltstones and shales of facies association F are interpreted as being deposited slightly below the SWB in the Jabal Akhdar and above it in the Huqf region, without recording fair weather structures. However, coarser grain size as well as a greater abundance of oscillatory structures suggests a shallower paleowater depth in the Huqf region. In the Huqf area facies association F of the Shuram Formation represents a significant increase of water depth compared to the peritidal environments of the Khufai Formation. The presence of storm-induced sedimentary structures in this deeper water facies association attests to an increased storm regime. This facies association, comprising the Middle Member, makes up the bulk of the Shuram Formation in the deeper-water Jabal Akhdar, but only a few tens of metres in the shallower-water Huqf area. A maximum flooding zone of the depositional sequence is located towards the base of the Middle Member, where it records minimum storm influence.

3.3.3. *Facies association G: clastic/carbonate parasequences*

In the Huqf area, facies association F gradationally passes upward into planar and swaley cross-stratified coarse siltstones with interbeds made of cross-stratified and wave-rippled ooidal grainstones containing intraformational clasts (G1; Table 1 and Fig. 9a). Storm-generated sedimentary structures such as climbing wave ripples, swaley cross-stratification, planar beds and edgewise conglomerates become more common upwards. Eventually this facies association develops into progressively thickening parasequences individually attaining a maximum of 20 m in thickness. The top of the Shuram Formation in the Jabal Akhdar also contains siliciclastic/carbonate m-scale cycles, though these are much finer grained than underlying stratigraphy and contain only rare evidence for storm reworking (edge-wise conglomerates) (G2; Table 1). They form m-scale symmetric and asymmetric cycles, before passing into the limestones at the base of the Buah Formation (Cozzi et al., 2004b).

The Huqf facies association G1 is interpreted as progressively thickening and shallowing upward parasequences of storm-dominated siltstones capped by ooidal grainstones deposited on a shallow shelf to shoreface, with water depths no greater than a few tens of metres. Facies association G2 in the Jabal Akhdar was deposited in an outer shelf environment with accumulation of thin-bedded siltstones below SWB.

Facies association G makes up the Upper Member of the Shuram Formation and gradationally passes upwards into the carbonate ramp succession of the Buah Formation (Cozzi et al., 2004b). In the Huqf area, parasequences gradually deepen upward, reaching a second order maximum flooding zone recognized by the presence of 10 m of monotonous shales marking the Shuram–Buah transition (Cozzi and Al-Siyabi, 2004; Cozzi et al., 2004b).

3.4. Regional depositional patterns

Thirty-two wells and regional seismic lines covering all of Oman (data provided by Petroleum Development Oman) have been interpreted in this study and integrated with field observations in order to document the regional depositional pattern across Oman. Wireline logs (gamma ray, neutron-bulk density, resistivity, etc.) as well as cuttings and core materials have been used to reconstruct the regional distribution of Shuram depositional facies. Based on this enlarged Shuram data set, individual wells have been classified into five different facies from deep to shallow water, with the Jabal Akhdar and Huqf as deep and shallow water end members, respectively (Fig. 12). Seismic profiles have been used to verify the lateral consistency of the well ties as well as to check depositional geometry, lateral thickness variations and the nature of the formation boundaries.

The Shuram Formation facies deepen from the Huqf area northward to the Jabal Akhdar and westward into the Ghaba Salt Basin. Farther to the west, the Makarem high marks another area of shallow water deposition. To the south of the Huqf outcrops, deep-water facies are encountered, before reaching shallow water facies again in the vicinity of Salalah in the Dhofar area (Fig. 12). This general pattern of deposition is consistent with those of the Masirah Bay and Khufai formations, though the quality of well coverage diminishes downwards in the lower part of the Nafun Group (Vroon-ten Hove, 1997; Romine et al., 2004; Fig. 13). This consistent trend during the deposition of the Nafun Group is at least in part inherited from the Fiq rifting event (Loosveld et al., 1996; Allen et al., 2004; Romine et al., 2004) since regional seismic and gravimetric surveys of basement show horst and graben structures (Loosveld et al., 1996; Romine et al., 2004). Abu Mahara (Fiq) rift basins strike roughly NE–SW, and appear to be cut by NW–SE oriented faults that are commonly attributed to the Najd trend of the Arabian shield (Fig. 13; Loosveld et al., 1996; Al-Husseini, 2000). The Nafun Group stratigraphy is thought to have been deposited during the thermal relaxation phase following Saqlah/Fiq-aged Abu Mahara rifting, its depocentres reflecting the inheritance of long-lived horsts and grabens in the Panafrican basement (Fig. 13).

3.5. Khufai–Shuram depositional model and sequence stratigraphic interpretation

The Khufai Formation displays a pattern of deposition consistent with a carbonate ramp setting (Fig. 6). A homoclinal ramp depositional model is preferred here to a distally steepened ramp (Read, 1985), as no seismic lines showing a sharp slope break and slope breccias, suggesting steep slopes, have been found in the deep-water Jabal Akhdar sections. The Khufai represents a shallowing-upward carbonate cycle (HST), from outer-ramp facies to cross-stratified grainstones and back-shoal mid-ramp deposits, to inner-ramp shallowing upward cycles (McCarron, 2000). The end of Khufai highstand deposition is marked, in the Jabal Akhdar, by small-incised channels, followed by a flooding into transgressive monotonous shales deposited below storm wave base (Fig. 11). However, in the Huqf region, the flooding is associated with the uppermost carbonate cycle or parasequence, followed by further deepening into storm-dominated siltstones deposited above storm wave base (Fig. 5). The Jabal Akhdar remained in deep water until progradation of the Buah carbonate ramp (Cozzi and Al-Siyabi, 2004; Cozzi et al., 2004b), whereas, the middle and upper members of the Shuram Formation in the Huqf area record progressive shoaling through a stack of shallowing upward storm-dominated parasequences (Fig. 5).

3.6. Khufai–Shuram chemostratigraphy

3.6.1. Materials and methods

Sixteen outcrop sections in the Jabal Akhdar and 16 sections in the Huqf area spanning the Khufai–Shuram boundary have been sampled, in the course of measuring stratigraphic sections, for inorganic carbon stable isotope analyses (about 700 measurements in total; two composite sections for the Jabal Akhdar and the Huqf area are shown in Table 2). Samples were drilled with 1–5 mm dental drill bits from freshly cut rock slabs avoiding sparry cement and vein material. The C and O isotope composition of powder from the carbonate samples were measured with a GasBench II connected to a Finnigan MAT DeltaPlus XL mass spectrometer, using a He-carrier gas system according to methods adapted after Spoetl and Vennemann (2003). Samples are normalized using an in-house standard calibrated against $\delta^{13}C$ and $\delta^{18}O$ values of NBS-19 (+1.95 and −2.20‰,

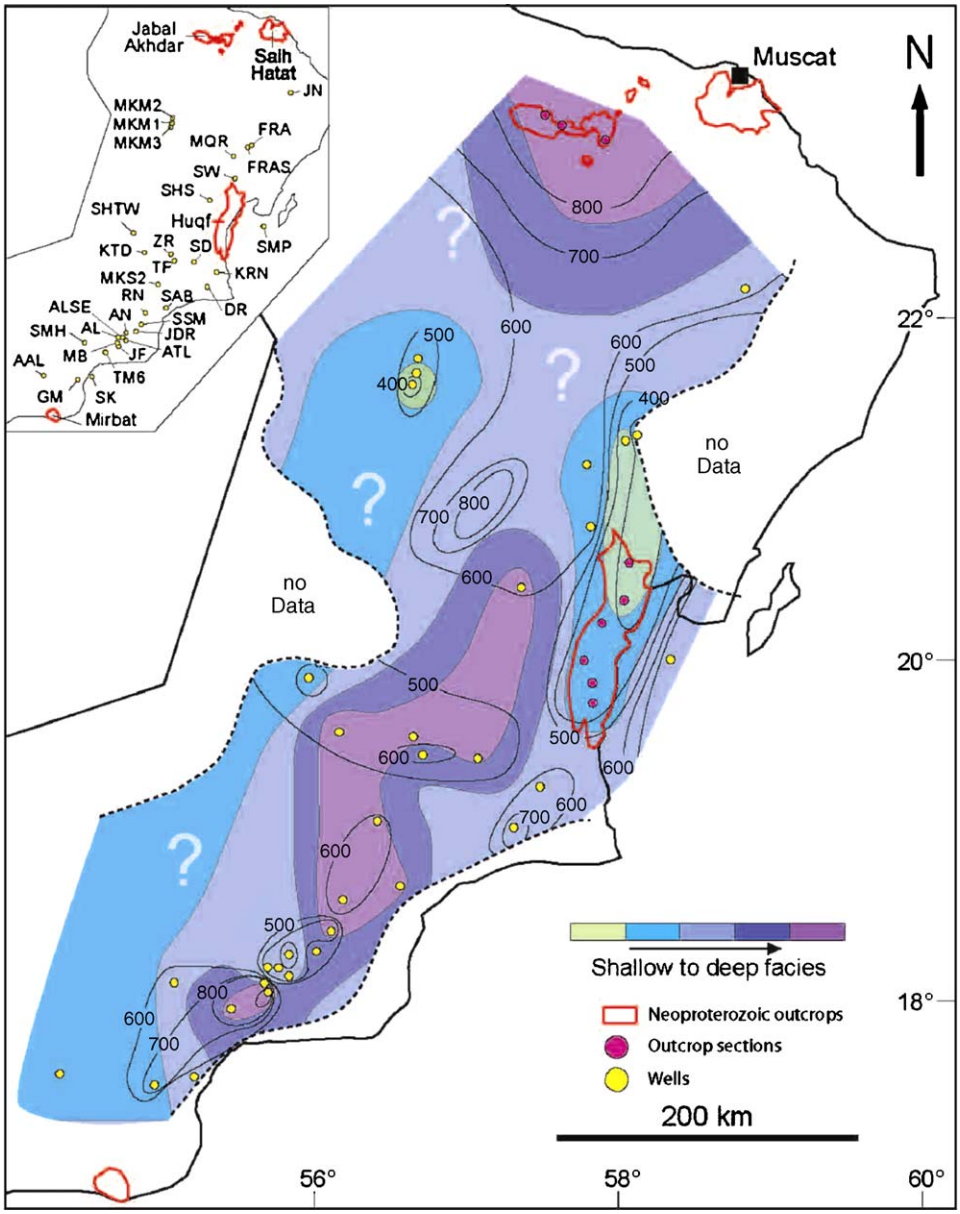

Fig. 12. Bathymetric facies and decompacted thickness map of the Shuram Formation in Oman. Decompaction was carried out using present-day burial depths for subsurface data, and a maximum burial depth of 4 km for outcrops, using initial porosities and porosity-depth coefficients for shales and carbonates. Map inset gives abbreviations of well names.

relative to VPDB). External reproducibility for the analyses estimated from replicate analyses of the in-house standard ($n = 6$) is ± 0.07‰ for $\delta^{13}C$ and ± 0.08‰ for $\delta^{18}O$.

3.7. Alteration

Some bulk carbonate samples were geochemically screened (Burns and Matter, 1993; Burns et al., 1994; McCarron, 2000; Leather, 2001). Elemental Sr, Mn and Fe were measured by McCarron (2000) on samples from Khufai, Shuram and Buah formations (Fig. 14A and B). The Mn/Sr ratio is a common proxy for diagenetic exchange. During meteoric diagenesis Sr is expelled from marine carbonate, whereas Mn is incorporated. However, absolute concentration of Sr, Mn and Fe reflects availability of reduced Sr, Mn and Fe in the original sea water or diagenetic fluid. The Mn–Sr plot for the carbonate of the Nafun Group shows no clear trend (Fig. 14B).

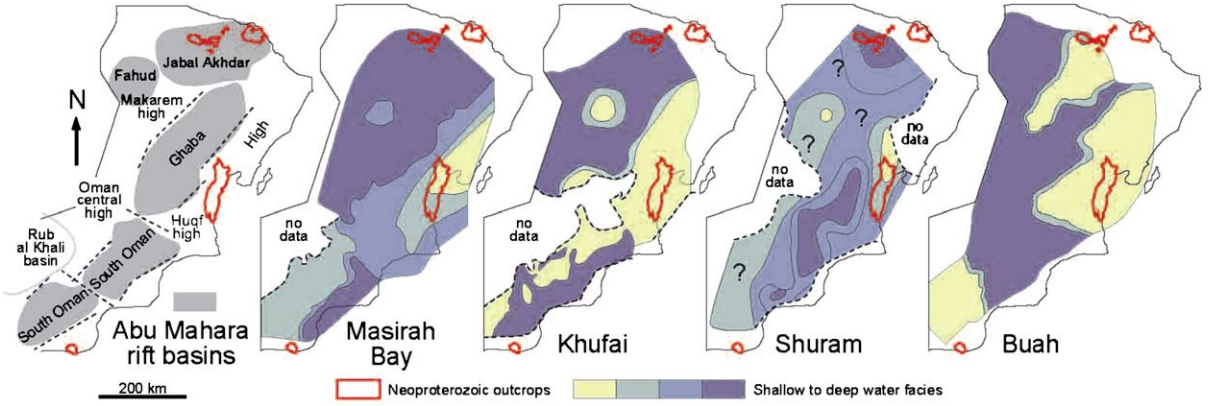

Fig. 13. Facies maps of the different formations of the Nafun Group and the Abu Mahara rift basins. Masirah Bay and Khufai maps are adapted after Allen and Leather (2006), Romine et al. (2004), Vroon-ten Hove (1997); Shuram map produced by this study; Buah map after Cozzi and Al-Siyabi (2004) and Abu Mahara rift general structure after Loosveld et al. (1996), Romine et al. (2004). Note the strong influence of the Abu Mahara basin structure on the deposition of all formations of the Nafun Group.

Samples have Mn/Sr ratios <10, with many samples <3, suggesting that most of the $\delta^{13}C$ and $\delta^{18}O$ values are not significantly diagenetically altered (Fig. 14C; Kaufman and Knoll, 1995). Additional isotopic data, which are consistent with the values in the samples screened for diagenetic alteration, were therefore used without further elemental screening.

When a plot of $\delta^{13}C$ versus $\delta\ ^{18}O$ (Fig. 14D) produces a straight line of positive slope, the covariance is thought to be due to meteoric alteration, which reduces both the carbon and oxygen isotopic ratios (Fairchild et al., 1990). In the Nafun Group excursion (samples ranging from top Khufai to Buah; i.e. from +5‰ down to −12‰ then back to +2‰), covariance R^2 is 0.461 for top Khufai plus Shuram samples in the Huqf area and 0.0010 for Jabal Akhdar samples. R^2 for Buah samples is 0.098 in the Huqf and 0.660 in the Jabal Akhdar. There is therefore no clear covariance between oxygen and carbon isotopic ratios, and the Shuram excursion is assumed to be negligibly affected by meteoric alteration.

Regional consistency between outcrop sections and well data, as well as geochemical screening for diagenetic alteration, confirm the authenticity of the chemostratigraphic trends (Burns and Matter, 1993; McCarron, 2000; Cozzi and Al-Siyabi, 2004; Cozzi et al., 2004a,b; Le Guerroué et al., 2006).

3.8. Results

The pattern of variation in $\delta^{13}C$ quickly rises from the negative (−5 to −3‰) Hadash cap carbonate values to positive values through the Masirah Bay Formation (∼+3‰, see data in Allen et al., 2004; Leather, 2001) and Khufai Formation (+4 to +5‰). Variation from the Khufai to the Buah Formations shows a positive–negative–positive cycle. Values around +4‰ characterize the top of the Khufai limestones, followed by a smooth decrease to zero within the last carbonate cycle (facies association C; Figs. 15 and 16). This smooth $\delta^{13}C$ isotopic decline is associated with a general minor shallowing at the top of the carbonate ramp from facies association B1 to C in the Huqf (Fig. 16) and from A2 to D in the Jabal Akhdar (Fig. 15). The decline to zero is followed by step-wise negative falls, at first to values of zero to −5‰, and then to values as negative as −12‰. The Jabal Akhdar section shows the two descending steps at the top and bottom boundaries of the Lower Member of the Shuram Formation (facies association E) (Table 2 and Fig. 15), whereas, the section in the Huqf shows this double stepped excursion at the boundaries of the uppermost carbonate cycle of the top Khufai ramp (facies association C) (Table 2 and Fig. 16). Based on this double chemostratigraphic step, the Khufai–Shuram boundary in the Jabal Akhdar is placed directly above the facies Db sandstone channels (or A2 facies when sandstones channels are missing; Fig. 11) and below the bleached siltstones of facies association E (Fig. 15). The uppermost Khufai carbonate parasequence in the Huqf area (facies association C) therefore correlates with the bleached siltstones (facies association E) of the Jabal Akhdar (Figs. 15 and 16). Although the Khufai–Shuram boundary marks the beginning of transgression, the top of the Lower Member of the Shuram Formation marks a more important transgressive event, which floods both the Jabal Akhdar and the Huqf areas to establish a relatively deep water sea (facies association F). Negative isotopic values persist throughout the Shuram Formation and into the base of the carbonates of the Buah

Table 2
Reference composite $\delta^{13}C$ and $\delta^{18}O$ isotope data of section 12 in the Jabal Akhdar and sections Na1, Na2 and MD5 in the Huqf region

Depth (m)	$\delta^{13}C$/VPDB	$\delta^{18}O$/VPDB
Jabal Akhdar 12		
110	−13.01	−6.07
107	−13.48	−5.52
103	−12.76	−3.47
102	−12.86	−4.28
98	−14.22	−6.90
97	−13.62	−6.73
96	−11.71	−4.04
93	−11.31	−4.07
87	−10.41	−6.38
81	−10.56	−3.40
80	−10.49	−0.78
76	−4.91	4.26
76	−4.77	5.96
68	−3.37	0.09
60	−6.01	2.32
59	−4.74	0.76
55	−5.36	2.59
53	−5.40	1.37
52	−2.86	−0.08
47	−2.98	2.21
43	−4.60	0.29
38	−2.53	0.09
35	−3.76	1.76
34	−2.46	−1.05
34	−3.01	−0.36
32	−1.93	−1.67
29	−2.42	0.23
28	−2.39	0.28
24	0.90	−0.59
24	0.87	−3.25
22	1.33	−3.04
22	1.72	−6.18
21	2.59	−6.59
19	2.06	−5.79
18	3.13	−6.22
17	2.13	−5.71
15	3.18	−6.02
13	3.84	−4.12
12	4.32	−2.85
10	4.51	−2.26
8	4.45	−2.92
6	5.73	−3.21
4	5.32	−4.00
3	5.03	−4.67
2	5.62	−4.21
0	5.10	−4.24
Huqf Na1		
300	−7.13	−8.29
295	−7.02	−8.41
290	−8.00	−8.62
283	−8.06	−8.91
271	−8.27	−8.78
265	−8.48	−8.94
258	−8.74	−8.92
251	−8.81	−9.27
247	−9.11	−9.09
221	−9.27	−8.78
211	−9.37	−8.88
202	−9.76	−8.78
Huqf Na2		
199	−9.01	−8.14
194	−9.27	−8.32
193	−9.22	−8.33
189	−9.19	−7.99
188	−9.46	−8.59
184	−9.42	−8.09
183	−9.46	−8.09
181	−9.58	−8.43
180	−9.70	−8.24
176	−9.78	−8.23
175	−9.75	−7.97
172	−10.04	−8.10
170	−10.18	−8.10
130	−10.64	−8.80
125	−10.89	−8.30
108	−11.83	−8.31
108	−11.84	−8.25
107	−11.94	−8.23
100	−12.05	−8.30
62	−12.81	−8.31
Huqf MD-18		
26	−7.66	−9.86
21	−7.73	−9.46
20	−7.02	−9.70
16	−6.69	−9.49
16	−6.08	−9.35
16	−6.09	−9.42
16	−5.06	−9.55
16	−4.15	−9.30
15	−4.16	−9.43
15	−4.08	−9.37
15	−4.02	−9.12
15	−3.91	−9.40
14	−3.97	−9.50
14	−3.96	−9.29
14	−3.66	−9.05
14	−3.53	−9.10
14	−2.60	−8.99
13	−0.71	−8.95
13	−0.94	−9.15
13	−0.45	−8.59
13	−1.15	−2.51
12	0.82	−2.66
12	0.52	−2.44
11	0.19	−2.70
11	0.47	−2.34
11	0.99	−1.53
10	0.97	−2.06
10	0.78	−2.78
9	0.83	−2.37

Table 2 (*Continued*)

Depth (m)	δ^{13}C/VPDB	δ^{18}O/VPDB
9	−0.07	−1.30
9	2.03	5.82
9	−3.09	1.72
7	0.20	−2.40
7	1.40	−2.01
6	1.25	5.35
5	3.87	3.67
4	2.53	4.39
2	4.46	3.00
0	4.50	3.02

Other isotopic data are found in Figs. 15 and 16.

Formation (−6‰), and then gradually climb back to positive values (+2‰; Cozzi et al., 2004a,b; Cozzi and Al-Siyabi, 2004) at the top of the Buah Formation. The Precambrian–Cambrian boundary in Oman is marked by a smaller negative excursion in the middle of the Ara Group (−3 to −5‰; Amthor et al., 2003).

It is critical to appreciate that the positive-negative-positive isotopic trend is regionally consistent and unbroken by offsets. This confirms the results of several region-wide sedimentological studies (Cozzi et al., 2004a; Cozzi and Al-Siyabi, 2004; McCarron, 2000) that failed to identify any major unconformities within the Nafun Group. Furthermore, carbon isotopic ratios show a systematic variation within a stack of parasequences near the top of the Shuram Formation in the Huqf area (facies G1), each cycle showing a trend in δ^{13}C in the direction of sedimentary progradation. This strongly suggests a long-term secular variation in δ^{13}C rather than a post-depositional overprint. These combined stratigraphic-carbon isotopic observations support a primary, oceanographic origin for the carbon isotopic ratios.

4. Implications for Ediacaran oceanography, paleoclimatology and correlation

4.1. Timing, duration and severity of the carbon cycle perturbation

Using a time transformation of the stratigraphic sections in Oman, based on the modelling of subsidence due to postrift thermal contraction (Le Guerroué et al., 2006), the major negative carbon isotopic excursion is interpreted to rapidly begin around ca. 600 Ma. The negative excursion continues with a steady rising limb crossing over to positive values at ca. 550 Ma. The negative excursion therefore has a duration of about 50 million years, starting some 35 My after the end of the Marinoan glacial

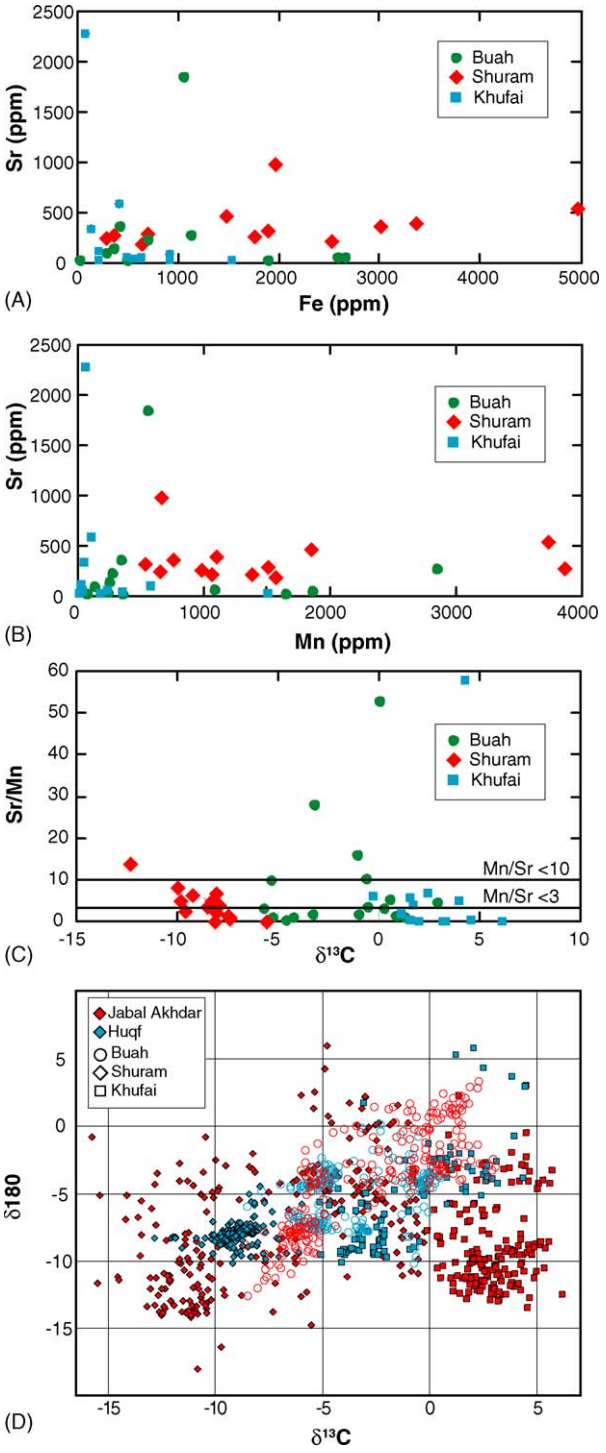

Fig. 14. (A–C) Elemental cross plots of carbonates from the Khufai, Shuram and Buah formations using Sr, Mn and Fe. After McCarron (2000). (D) δ^{13}C vs. δ^{18}O covariance plot. Data from this study and Cozzi et al. (2004b).

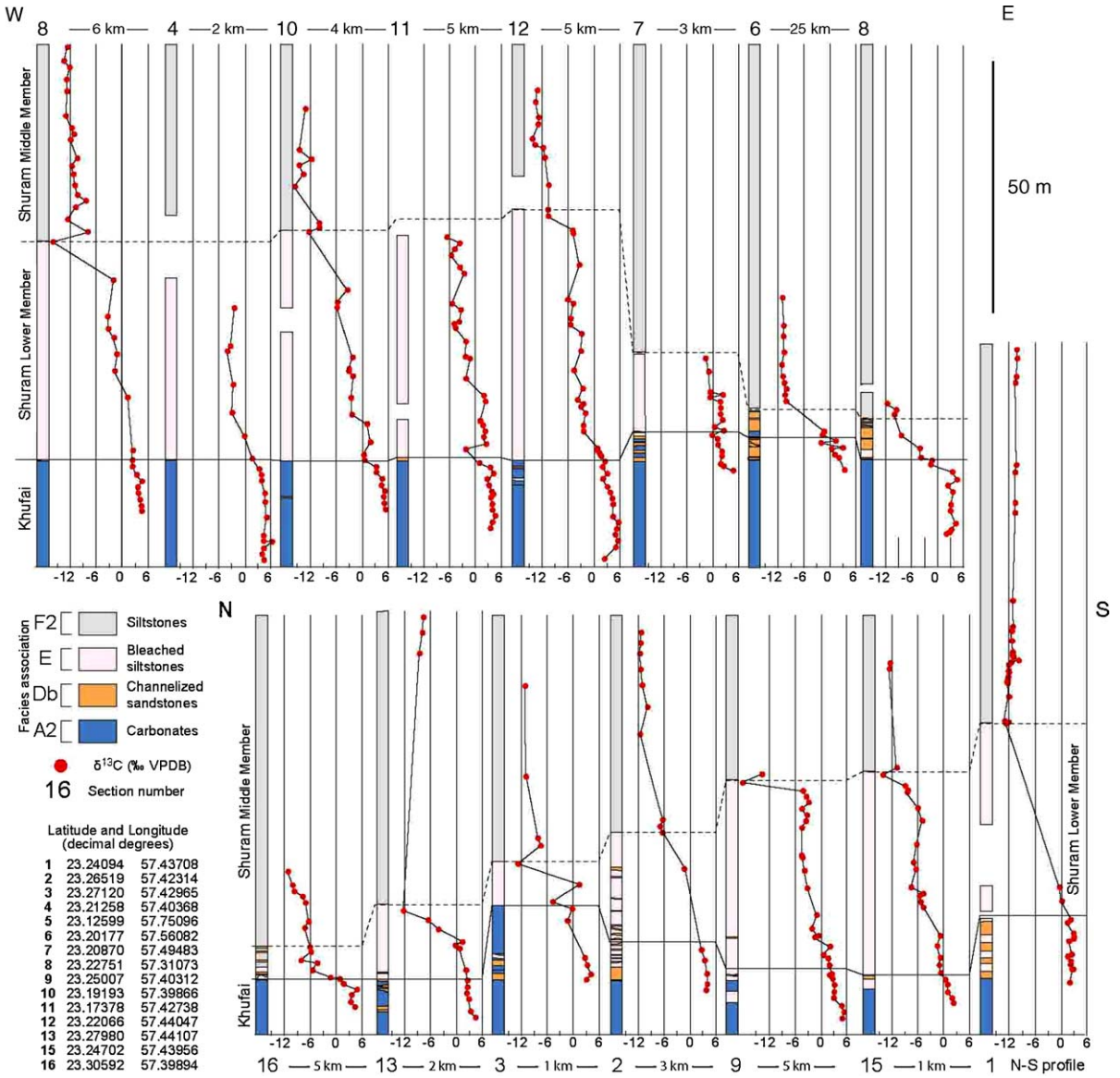

Fig. 15. Carbon isotope data plotted against simplified sedimentary logs around the Khufai–Shuram boundary in the Jabal Akhdar. East-west and north-south profiles. Note the slow decrease of $\delta^{13}C$ in the uppermost Khufai as well as the two drops at the base and top of the bleached siltstones of the Shuram Lower Member.

epoch, dated in Namibia at 635.5 ± 0.6 Ma (Hoffmann et al., 2004) and at 635.2 ± 0.6 Ma in south China (Condon et al., 2005), and ending less than 10 My before the Precambrian–Cambrian boundary (542 Ma; Amthor et al., 2003). A $\delta^{13}C_{carb}$ excursion of this amplitude and duration is unique in Earth history.

4.2. Worldwide correlation of the $\delta^{13}C$ excursion

Ediacaran strata recording negative $\delta^{13}C_{carb}$ values similar to those of the Khufai–Shuram boundary in Oman are found in the Wonoka Formation of the Adelaide Rift Complex of South Australia (Gostin and Jenkins, 1983; Preiss, 1987; Calver, 2000), the Johnnie Formation of the Death Valley region of western USA (Christie-Blick and Levy, 1989; Corsetti and Hagadorn, 2000; Corsetti and Kaufman, 2003), the Doushantuo Formation of south China (Condon et al., 2005), the Chenchinskaya, Nikolskaya and Torginskay Formations of Siberia (Melezhik et al., 2005) and the Krol Group of northern India (Jiang et al., 2002). However, these possible correlatives have a limited $\delta^{13}C$ dataset and are

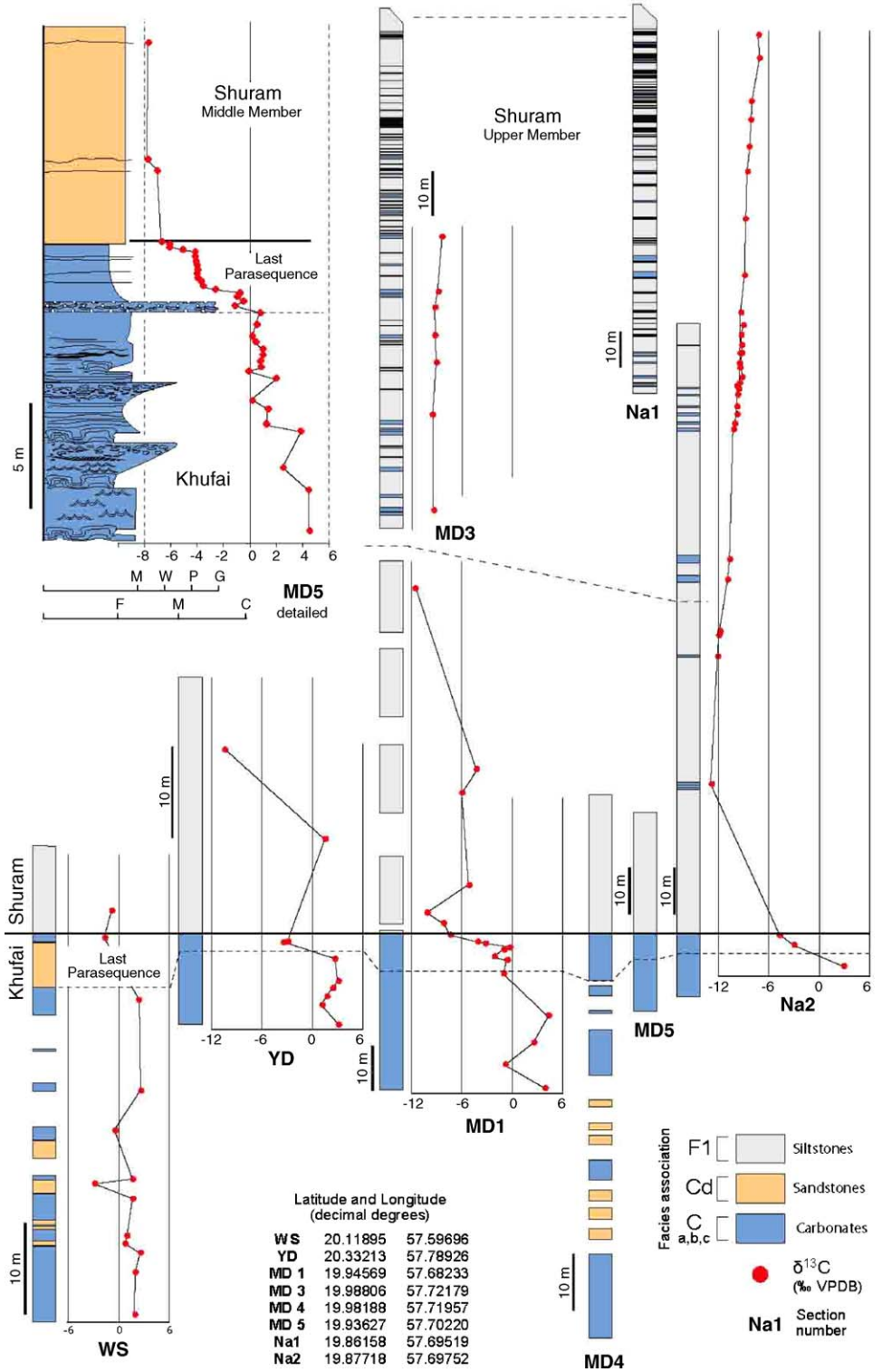

Fig. 16. Carbon isotope data plotted against simplified sedimentary logs around the Khufai–Shuram boundary in the Huqf area. Note the detailed MD5 section that shows the two-step drop of $\delta^{13}C$ associated with the last parasequence of the Khufai Formation, and the slow decrease of $\delta^{13}C$ in the uppermost Khufai Formation.

dissected by unconformities, so that the full excursion cannot be recognized. The Doushantuo probably records the end of the excursion at around ca. 551 Ma (Condon et al., 2005; Le Guerroué et al., 2006).

Although the Windermere Supergroup of Canada contains two grand cycles that appear to correlate with the Nafun Group of Oman, and strontium isotopes (Narbonne et al., 1994) support a correlation of the Blueflower and Shuram Formations (Le Guerroué et al., 2006), the carbon isotopic data from the Windermere section (Narbonne et al., 1994) do not replicate the Shuram shift. Similarly, the Jiucheng member of south China (Kimura et al., 2005), which is a possible Shuram equivalent, does not bear a carbon isotopic excursion in carbonate of comparable magnitude to the Shuram shift.

4.3. Gaskiers' and equivalent glaciations

Glaciation during Ediacaran times is commonly accepted and recognized as the Varangerian/Gaskiers event (Halverson et al., 2005). Age constraints on glaciation remain a highly debated issue since only sparse absolute ages are available. Nevertheless, the best constraint on a post-Marinoan event is given by the Gaskiers glaciation of Newfoundland (Krogh et al., 1988), which is precisely dated at 580 Ma and lasted less than 1 My (Bowring et al., 2003). Coeval glacial deposits are also found in the Boston basin, where the Squantum Formation is bracketed to between 590 and 575 Ma (Thompson and Bowring, 2000), though its glacial origin is debated (Eyles and Januszczak, 2004). Similar ages obtained on the Loch na Cille Boulder Bed in Scotland (Elles, 1934) and equivalent beds in Ireland (Condon and Prave, 2000), constrained to be younger than 601 ± 4 Ma (Dempster et al., 2002), are in accord with the age of the Gaskiers glaciation. Other constraints are given by the Cottons Breccia and equivalent Croles Hill Diamictite to 582 ± 4 and 574.7 ± 3 Ma, respectively (Calver et al., 2004). Finally, the Olympic and Inishowen ice-rafted debris are both constrained to be $<592 \pm 14$ Ma (Re–Os age; Schaefer and Burgess, 2003) and ca. 590–570 Ma (Condon and Prave, 2000), respectively. However, the Olympic is considered to be Marinoan aged (ca. 635; Halverson et al., 2005). Ediacaran glaciation is therefore thought to have occurred around 580 Ma and to have lasted a short time (Halverson et al., 2005), unlike postulated snowball Earth events (Hoffman et al., 1998).

The short-lived Gaskiers glaciation is therefore embedded within a much longer time period occupied by the Shuram Formation $\delta^{13}C$ excursion. The isotopic excursion appears to have begun and ended independently of glaciation. Consequently, any link between the Shuram excursion and the negative $\delta^{13}C$ values of carbonates bracketing Gaskiers-aged glacial deposits in Newfoundland (Myrow and Kaufman, 1999), the Quruqtagh Formation in northwest China (Xiao et al., 2004), and the Mortensnes Formation in Svalbard (Edwards, 1984) could be coincidental. If our chronology is incorrect and the sharp fall in carbon isotopic values at the Khufai–Shuram boundary correlates in time with the shortlived and localized 580 Ma Gaskiers glaciation, the amplitude of the excursion and subsequent recovery through 1 km of stratigraphy, crossing over to positive values at ca. 550 Ma, would still be unexplained. There is consequently no justification for linking the Shuram carbon isotopic excursion to the Gaskiers event.

4.4. Climate change and oceanography

Neoproterozoic carbonates record highly negative $\delta^{13}C$ values of strongly debated origin (Christie-Blick et al., 1995; Kaufman and Knoll, 1995; Kaufman et al., 1997; Hayes et al., 1999; Walter et al., 2000; Hoffman and Schrag, 2002; Schrag et al., 2002; Halverson et al., 2005).

The precipitation of isotopically depleted cap carbonates is explained in the snowball Earth theory by the prior build-up of mantle-derived carbon in the atmosphere–ocean reservoir during a period of prolonged hydrological shutdown during which silicate weathering was inoperative (Hoffman et al., 1998). This model is not applicable to the Shuram anomaly since the latter is unrelated to glaciation, and, furthermore, expected $\delta^{13}C$ values in co-precipitated carbonates cannot reach values lower than the -5 to $-6‰$ $\delta^{13}C$ values typical of mantle sources (Des Marais and Moore, 1984).

The depleted values of Neoproterozoic carbonates may also be explained by the action of a biological pump in a stratified ocean (Grotzinger and Knoll, 1995; Kaufman et al., 1997). Turnover of the deep-water, $\delta^{13}C$-depleted reservoir during deglaciation would cause the precipitation of carbonates with light $\delta^{13}C$ values in shallow water. Interestingly, Shen et al. (2005) reported a possible carbon isotopic gradient of ~3‰ along a paleoenvironmental transect from shelf to deep basinal sedimentary facies in the Marinoan Nantuo cap carbonate. However, with regard to the Shuram anomaly, no lateral gradient is decipherable between the $\delta^{13}C$ data sets from shallow and deep-water facies (compare Figs. 15 and 16). In addition, this model cannot explain values as negative as $-12‰$.

It has also been proposed that negative carbon isotopic ratios in carbonate might reflect flows from a light carbon

reservoir such as methane hydrates/clathrates, either in the form of seabed hydrates or in terrestrial permafrost (Kvenvolden, 1998; Kennedy et al., 2001; Jiang et al., 2003; Kasemann et al., 2005). This mechanism has been invoked to explain the highly variable and very negative values of the Doushantuo 'cap carbonate' in south China (down to −5‰; Jiang et al., 2003). Schrag et al. (2002) also believed that a large oceanic methane reservoir was slowly released, having built up through high amounts of organic carbon burial due to high river discharges from continental areas assembled at low latitude. In the case of the Shuram anomaly, the severity of the $\delta^{13}C$ perturbation and its protracted steady recovery towards positive values make it unlikely that these mechanisms acted as the main driver of the Shuram anomaly.

Shields (2005) envisaged extensive (global) freshwater plumes caused by melting of ice caps during catastrophic deglaciation, but did not consider the impact of the plume world on carbon isotopic ratios in marine carbonate. The Shuram anomaly is clearly unrelated to any direct glacial influence, although the Shuram ocean may have been subject to major influxes of fresh water during a climatic change to pluvial conditions (see also Le Guerroué et al., 2006).

Rothman et al. (2003) used geochemical modelling to suggest that fluctuation in the size of the reservoir of dissolved organic carbon in ocean water or changes in the fractionation associated with organic production would lead to major variations in the isotopic record. Pulses in the remineralization (enhanced by glaciation) or bioremineralization (enhanced by early metazoans) of a large oceanic organic carbon pool could potentially explain the negative excursions recorded by Neoproterozoic carbonates. However, such a carbon pool remains to be physically identified. The Shuram anomaly conclusively shows that mantle input is insufficient to generate −12‰ values and probably oxidation of organic matter (around −25 to −30‰; Hayes et al., 1999) is required. Rothman et al.'s (2003) non steady-state model demonstrates that long and severe negative perturbations are possible and most likely linked with evolution of the biosphere during the Neoproterozoic (see also Grey et al., 2003). Slow remineralisation might be reflected in the steady recovery of the negative anomaly.

All of these hypotheses have elements that may go some way to explaining the Shuram shift. However, with the possible exception of Rothman et al.'s (2003) hypothesis of remineralization of dissolved organic carbon, they have difficulty in explaining the extremely long duration of the negative excursion. Others cannot explain the extremely negative isotopic values. There are a number of linked elements in the models so far proposed, including high rates of organic carbon burial, anoxic ocean waters, release of large methane reservoirs, and remineralization of dissolved organic carbon.

In summary, the cause, or causes, of the Shuram shift remain enigmatic, but any explanation must be guided by a number of pertinent observations: (1) the carbon isotopic excursion is in phase with relative sea level, effectively occupying the second grand cycle of the Nafun Group; (2) the onset of the fall in $\delta^{13}C$ corresponds with the demise of the Khufai carbonate factory and the influx of siliciclastics onto the carbonate ramp; (3) the nadir of the carbon isotopic excursion corresponds with a period of maximum flooding, so the period of fall of carbon isotopic values roughly approximates the period of transgression; (4) the sedimentology of the Shuram Formation in the Huqf area demonstrates that the Shuram marine basin was typified by high energy storm conditions; (5) the change from Khufai to Shuram most likely corresponds to a change from arid to pluvial-humid conditions.

5. Conclusions

The Nafun Group of the Huqf Supergroup of Oman records an essentially continuous period of deposition from the post-Marinoan cap carbonate of the Hadash Formation to close to the Precambrian–Cambrian boundary. It comprises two grand cycles of marine siliciclastics to ramp carbonates. Each cycle is initiated by a major transgression, the formation of a relatively deep siliciclastic marine basin, followed by gradual shallowing up into progradational ramp carbonates.

The boundary between the two grand cycles is at the Khufai–Shuram boundary. Both the Khufai and Shuram Formations are represented by shallow water facies in the Huqf area of east-central Oman, and by deeper water facies in the Jabal Akhdar of north Oman. In the Huqf area, the Khufai Formation is composed of fetid carbonates, which pass up into m-scale peritidal cycles, indicating progradation of a carbonate ramp. In the Jabal Akhdar, however, the Khufai Formation is dominated by black, pyritic limestones deposited in deeper ramp conditions. The Shuram Formation is composed of storm-influenced sandstones, siltstones and limestones in the relatively shallow water Huqf area. In the Jabal Akhdar, however, the Shuram Formation is dominated by deep water, organic-rich dolomitic mudstones and bleached siltstones at the base, which pass up into very thick, purple, monotonous siltstones and shales with thin subordinate carbonates. Shallow water conditions were established over basement highs, which may have been partially inherited from a phase of

important rifting during the deposition of the underlying Abu Mahara Group.

The carbonates of the upper grand cycle, comprising the Shuram and Buah Formations, contain a remarkable negative excursion in $\delta^{13}C$ values, which start to fall precipitously from the uppermost Khufai Formation, reach a nadir close to the maximum flooding zone of the Shuram, and then recover monotonically through nearly 1 km of stratigraphy, with a crossing point within the Buah Formation. The amplitude of the excursion is from +5‰ in the Khufai carbonates, to −12‰ in the lower Shuram Formation, and the duration is believed to be ca. 50 My. This appears to be the greatest $\delta^{13}C$ negative excursion in inorganic carbon of marine carbonates of Earth history.

The explanation for the Shuram shift is enigmatic. However, there are a number of pointers derived from the sedimentology and stratigraphy of the Nafun Group. Importantly, the carbon isotopic excursion is roughly in phase with relative sea level. The start of the fall in carbon isotopic values commences with the influx of siliciclastics and the demise of the Khufai carbonate factory, and the nadir occurs at the level of the maximum flooding zone of the lower Shuram, so the falling segment of the excursion coincides with a period of transgression. We also note that the transition from the Khufai to the Shuram Formation most likely records a climate change from arid to humid and stormy.

Acknowledgements

We are extremely grateful for the long-term logistical and financial assistance of Petroleum Development Oman, and to the Ministry of Oil and Gas of Oman for permission to publish the borehole data. Erwan Le Guerroué was funded by ETH-Zürich (TH-Projekt Nr. TH-1/02-3). We thank Gretta McCarron for preliminary work leading to this study, and Alex Wyss, Benjamin Le Bayon and Matthias Papp for help in the field. Carbon isotope measurements were made in Torsten Vennemann's laboratory at University of Lausanne. James Etienne, Galen Halverson, Martin Kennedy, John Grotzinger, Ruben Rieu and David Fike are thanked for their useful ongoing discussions. Several staff at Petroleum Development Oman (PDO) are also thanked for their logistical help and technical input, including Jan Schreurs, Hisham al Siyabi, Joachim Amthor and Mark Newall. We are grateful to Galen Halverson and an anonymous reviewer for their comments on the manuscript.

References

Al-Husseini, M.I., 2000. Origin of the Arabian plate structures: Amar collision and Najd rift. GeoArabia 5 (4), 527–542.

Allen, P.A., 1981. Some guidelines in reconstructing ancient sea conditions from wave ripple marks. Marine Geol. 43, M59–M67.

Allen, P.A., 1984. Reconstruction of ancient sea conditions with an example from the Swiss Molasse. Marine Geol. 60, 455–473.

Allen, P.A., Leather, J., 2006. Post-Marinoan marine siliciclastic sedimentation: the Masirah Bay Formation, Neoproterozoic Huqf Supergroup of Oman. Precambrian Res. 144, 167–198.

Allen, P.A., Hoffman, P.F., 2005. Extreme winds and waves in the aftermath of a Neoproterozoic glaciation. Nature 433 (7022), 123–127.

Allen, P.A., Leather, J., Brasier, M.D., 2004. The Neoproterozoic Fiq glaciation and its aftermath, Huqf Supergroup of Oman. Basin Res. 16 (4), 507–534.

Amthor, J.E., et al., 2003. Extinction of *Cloudina* and *Namacalathus* at the Precambrian–Cambrian boundary in Oman. Geology 31 (5), 431–434.

Beurrier, M., Béchennec, F., Rabu, R., Hutin, G., 1986. Geological map of Rustaq, Sheet NF 40-3D, scale 1:100,000. Directorate General of minerals, Oman ministry of petroleum and minerals.

Bowring, S., Myrow, P., Landing, E., Ramezani, J., Grotzinger, J., 2003. Geochronological constraints on terminal Neoproterozoic events and the rise of Metazoans. Geophys. Res. Abstr. 5, 13219.

Brasier, M., et al., 2000. New U–Pb zircon dates for the Neoproterozoic Ghubrah glaciation and for the top of the Huqf Supergroup, Oman. Geology 28 (2), 175–178.

Burns, S.J., Haudenschild, U., Matter, A., 1994. The strontium isotopic composition of carbonates from the late Precambrian (~560–540 Ma) Huqf Group of Oman. Chem. Geol. 111 (1–4), 269–282.

Burns, S.J., Matter, A., 1993. Carbon isotopic record of the latest Proterozoic from Oman. Eclogae Geologicae Helvetiae 86 (2), 595–607.

Calver, C.R., 2000. Isotope stratigraphy of the Ediacaran (Neoproterozoic III) of the Adelaide rift complex, Australia, and the overprint of water column stratification. Precambrian Res. 100, 121–150.

Calver, C.R., Black, L.P., Everard, J.L., Seymour, D.B., 2004. U–Pb zircon age constraints on late Neoproterozoic glaciation in Tasmania. Geology 32 (10), 893–896.

Christie-Blick, N., Dyson, I.A., von der Borch, C.C., 1995. Sequence stratigraphy and the interpretation of Neoproterozoic earth history. Precambrian Res. 73 (1–4), 3–26.

Christie-Blick, N., Levy, M., 1989. Stratigraphic and tectonic framework of upper Proterozoic and Cambrian rocks in the Western United States. In: Christie-Blick, N., Levy, M., Mount, J.F., Signor, P.W., Link, P.K. (Eds.), Proceedings of the 28th International Geological Congress Field Trip Guidebook T331 on Late Proterozoic and Cambrian tectonics, sedimentation, and record of metazoan radiation in the Western United States. American Geophysical Union, pp. 7–22.

Condon, D., et al., 2005. U–Pb ages from the Neoproterozoic Doushantuo Formation, China. Science 308, 95–98.

Condon, D.J., Prave, A.R., 2000. Two from Donegal: Neoproterozoic glacial episodes on the northeast margin of Laurentia. Geology 28 (10), 951–954.

Corsetti, F.A., Hagadorn, J.W., 2000. Precambrian–Cambrian transition: Death Valley, United States. Geology 28 (4), 299–302.

Corsetti, F.A., Kaufman, A.J., 2003. Stratigraphic investigations of carbon isotope anomalies and Neoproterozoic ice ages in Death Valley, California. Geol. Soc. Am. Bull. 115 (8), 916–932.

Cozzi, A., Al-Siyabi, H.A., 2004. Sedimentology and play potential of the late Neoproterozoic Buah Carbonates of Oman. GeoArabia 9 (4), 11–36.

Cozzi, A., Allen, P.A., Grotzinger, J.P., 2004a. Understanding carbonate ramp dynamics using $\delta^{13}C$ profiles: examples from the Neoproterozoic Buah Formation of Oman. Terra Nova 16 (2), 62–67.

Cozzi, A., Grotzinger, J.P., Allen, P.A., 2004b. Evolution of a terminal Neoproterozoic carbonate ramp system (Buah Formation, Sultanate of Oman): Effects of basement paleotopography. Geol. Soc. Am. Bull. 116 (11/12), 1121–1131.

Dempster, T.J., et al., 2002. Timing of deposition, orogenesis and glaciation within the Dalradian rocks of Scotland: constraints from U–Pb zircon ages. J. Geol. Soc., Lond. 159, 83–94.

Des Marais, D.J., Moore, J.G., 1984. Carbon and its isotopes in mid-oceanic basaltic glasses. Earth Planet. Sci. Lett. 69, 43–57.

Dubreuilh, J. et al., 1992. Geological map of Khaluf, Sheet NF 40-15, scale 1:250,000. Directorate General of minerals, Oman ministry of petroleum and minerals.

Dumas, S., Arnott, R.W.C., Southard, J.B., 2005. Experiments on oscillatory-flow and combined-flow bed forms: Implications for interpreting parts of the shallow-marine sedimentary record. J. Sedimen. Res. 75 (3), 501–513.

Edwards, M.B., 1984. Sedimentology of the Upper Proterozoic glacial record, Vestertan Group, Finnmark, North Norway. Norges Geologiske Undersøkelse 384, 1–76.

Elles, G., 1934. The Loch na Cille Boulder Bed and its place in the Highland Succession. Quart. J. Geol. Soc. 91, 111–147.

Eyles, N., Januszczak, N., 2004. 'Zipper-rift': a tectonic model for Neoproterozoic glaciations during the breakup of Rodinia after 750 Ma. Earth Sci. Rev. 65 (1/2), 1–73.

Fairchild, I.J., Marshall, J.D., Bertrand-Sarfati, J., 1990. Stratigraphic shifts in carbon isotopes from Proterozoic stromatolitic carbonates (Mauritania): influences of primary mineralogy and diagenesis. Am. J. Sci. 290 (A), 46–79.

Galli, M.T., Jadoul, F., Bernasconi, S.M., Weissert, H., 2005. Anomalies in global carbon cycling and extinction at the Triassic/Jurassic boundary: evidence from a marine C-isotope record. Palaeogeogr. Palaeoclimatol. Palaeoecol. 216 (3/4), 203–214.

Glennie, K.W., et al., 1974. Geology of the Oman Mountains. Verhandelingen van het Koninklijk Nederlands geologisch mijnbouwkundig Genootschap 31, 423.

Gorin, G.E., Racz, L.G., Walter, M.R., 1982. Late Precambrian–Cambrian sediments of Huqf Group, Sultanate of Oman. Am. Assoc. Petrol. Geol. Bull. 66 (12), 2609–2627.

Gostin, V.A., Jenkins, R.J.F., 1983. Sedimentation of the early Ediacaran, Flinders Ranges, South Australia. Geol. Soc. Austr. Abstr. 9, 196–197.

Grey, K., Walter, M.R., Calver, C.R., 2003. Neoproterozoic biotic diversification: snowball Earth or aftermath of the Acraman impact? Geology 31, 459462.

Grotzinger, J.P., Knoll, A.H., 1995. Anomalous carbonate precipitates: is the Precambrian the key to the Permian? Palaios 10, 578–596.

Halverson, G.P., Hoffman, P.F., Schrag, D.P., Maloof, A.C., Rice, A.H.N., 2005. Towards a Neoproterozoic composite carbon isotope record. Geol. Soc. Am. Bull. 117 (9/10).

Hayes, J.M., Strauss, H., Kaufman, A.J., 1999. The abundance of 13C in marine organic matter and isotopic fractionation in the global biogeochemical cycle of carbon during the past 800 Ma. Chem. Geol. 161 (1–3), 103–125.

Hesselbo, S.P., et al., 2000. Massive dissociation of gas hydrate during a Jurassic oceanic anoxic event. Nature 406 (6794), 392–395.

Hoffman, P.F., Kaufman, A.J., Halverson, G.P., Schrag, D.P., 1998. A Neoproterozoic snowball earth. Science 281 (5381), 1342–1346.

Hoffman, P.F., Schrag, D.P., 2002. The snowball Earth hypothesis: testing the limits of global change. Terra Nova 14 (3), 129–155.

Hoffmann, K.H., Condon, D.J., Bowring, S.A., Crowley, J.L., 2004. U–Pb zircon date from the Neoproterozoic Ghaub Formation, Namibia: Constraints on Marinoan glaciation. Geology 32 (9), 817–820.

Hughes-Clarke, M.W., 1988. Stratigraphy and rock nomenclature in the oil-producing area of interior Oman. J. Petrol. Geol. 11 (1), 5–60.

Jiang, G.Q., Christie-Blick, N., Kaufman, A.J., Banerjee, D.M., Rai, V., 2002. Sequence stratigraphy of the Neoproterozoic Infra Krol Formation and Krol Group, Lesser Himalaya, India. J. Sediment. Res. 72, 524–542.

Jiang, G., Kennedy, M.J., Christie-Blick, N., 2003. Stable isotopic evidence for methane seeps in Neoproterozoic postglacial cap carbonates. Nature 426 (6968), 822–826.

Kapp, H.E., Llewellyn, P.G., 1965. The geology of the Central Oman Mountains. Report S00005-9, geological group, Petroleum Development Oman Ltd.

Kasemann, S.A., Hawkesworth, C.J., Prave, A.R., Fallick, A.E., Pearson, P.N., 2005. Boron and calcium isotope composition in Neoproterozoic carbonate rocks from Namibia: evidence for extreme environmental change. Earth Planet. Sci. Lett. 231 (1/2), 73–86.

Kassler, P., 1965. The Geology of the Haushi, Central Huqf and Masirah Island areas (Southern Oman). Petroleum Development Oman Ltd., Doha Geologial Group, 19.

Kaufman, A.J., Knoll, A.H., 1995. Neoproterozoic variations in the C-isotopic composition of seawater: Stratigraphic and biogeochemical implications. Precambrian Res. 73, 27–49.

Kaufman, A.J., Knoll, A.H., Narbonne, G.M., 1997. Isotopes, ice ages, and terminal Proterozoic earth history. Proc. Natl. Acad. Sci. U.S.A. 94 (13), 6600–6605.

Kennedy, M.J., Christie-Blick, N., Sohl, L.E., 2001. Are Proterozoic cap carbonates and isotopic excursions a record of gas hydrate destabilization following Earth's coldest intervals? Geology 29 (5), 443–446.

Kimura, H., Azmy, K., Yamamuro, M., Zhi-Wen, J., Cizdziel, J.V., 2005. Integrated stratigraphy of the upper Neoproterozoic succession in Yunnan Province of South China: re-evaluation of global correlation and carbon cycle. Precambrian Res. 138 (1/2), 1–36.

Knoll, A.H., Walter, M.R., Narbonne, G.M., Christie-Blick, N., 2004. A new period for the geologic time scale. Science 305 (5684), 621–622.

Krogh, T.E., Strong, D.F., O'Brien, S.J., Papezik, V., 1988. Precise U–Pb zircon dates from the Avalon Terrane in Newfoundland. Can. J. Earth Sci. 25, 442–453.

Kvenvolden, K.A., 1998. A primer on the geological occurrence of gas hydrate. In: Henriet, J.-P., Mienert, J. (Eds.), Gas Hydrates: Relevance to World Margin Stability and Climate Change, 137. Geological Society of London Special Publication, pp. 9–30.

Le Guerroué, E., Allen, P.A., Cozzi, A., 2005. Two distinct glacial successions in the Neoproterozoic of Oman. GeoArabia 10 (2), 17–34.

Le Guerroué, E., Allen, P.A., Cozzi, A., Fanning, C.M., 2006. Fifty million year duration negative carbon isotopic excursion in the Ediacaran ocean. Terra Nova, in press.

Leather, J., 2001. Sedimentology, Chemostratigraphy, and Geochronology of the Lower Huqf Supergroup, Oman. Unpublished PhD Dissertation, Trinity College Dublin, 275.

Leather, J., Allen, P., Brasier, M., Cozzi, A., 2002. Neoproterozoic snowball Earth under scrutinity: Evidence from the Fiq glaciation of Oman. Geology 30 (10), 891–894.

Loosveld, R.J.H., Bell, A., Terken, J.J.M., 1996. The tectonic evolution of interior Oman. GeoArabia 1 (1), 28–50.

McCarron, G.M.E., 2000. The sedimentology and chemostratigraphy of the Nafun Group, Huqf Supergroup, Oman. Unpublished PhD Dissertation, Oxford University, 175.

Melezhik, V.A., Fallick, A.E., Pokrovsky, B.G., 2005. Enigmatic nature of thick sedimentary carbonates depleted in ^{13}C beyond the canonical mantle value: The challenges to our understanding of the terrestrial carbon cycle. Precambrian Res. 137 (3/4), 131–165.

Nicholas, C.J., Brasier, M., 2000. Outcrop equivalent of the subsurface Precambrian–Cambrian Ara Group in Oman. In: Proceedings of the Fourth Middle East Geosciences Conference, GEO 2000, vol. 5, GeoArabia, pp. 151–152 (Abstract).

Myrow, P.M., Kaufman, A.J., 1999. A newly discovered cap carbonate above Varanger-age glacial deposits in Newfoundland. Can. J. Sedimen. Res. 69, 784–793.

Narbonne, G.M., Kaufman, A.J., Knoll, A.H., 1994. Integrated chemostratigraphy and biostratigraphy of the Windermere Supergroup, northwestern Canada: implications for Neoproterozoic correlations and the early evolution of animals. Geol. Soc. Am. Bull. 106, 1281–1292.

Platel, J.P. et al., 1992. Geological map of Duqm and Madraca, sheet NE 40-03/07, scale 1:250,000. Directorate General of minerals, Oman ministry of petroleum and minerals.

Preiss, W.V., 1987. The Adelaide Geosyncline late Proterozoic stratigraphy, sedimentation, palaeontology and tectonics. Geol. Survey South Austr. Bull. 53, 438.

Rabu, D., 1988. Géologie de l'autochtone des montagnes d'Oman, la fenêtre du Jabal Akhdar. Thèse Doct. ès-Sciences, Univ. of P. et M. Curie, Paris 6, and documents BRGM, 130.

Read, J.F., 1985. Carbonate platform facies models. Am. Assoc. Petrol. Geol. Bull. 69, 1–21.

Romine, K. et al., 2004. North Oman Haima-Huqf Tectonostratigraphy Study. SRK Confidential Report to PDO.

Rothman, D.H., Hayes, J.M., Summons, R.E., 2003. Dynamics of the Neoproterozoic carbon cycle. Proc. Natl. Acad. Sci. U.S.A. 10 (14), 8124–8129.

Schaefer, B.F., Burgess, J.M., 2003. Re–Os isotopic age constraints on deposition in the Neoproterozoic Amadeus Basin: implications for Snowball Earth. J. Geol. Soc., Lond. 160, 825–828.

Schrag, D.P., Berner, R.A., Hoffman, P.F., Halverson, G.P., 2002. On the initiation of a snowball Earth. Geochem. Geophys. Geosyst. 3 (Art. no. 1036).

Shen, Y., Zhang, T., Chu, X., 2005. C-isotopic stratification in a Neoproterozoic postglacial ocean. Precambrian Res. 137 (3/4), 243–251.

Shields, G.A., 2005. Neoproterozoic cap carbonates: a critical appraisal of existing models and the plumeworld hypothesis. Terra Nova 17 (4), 299–310.

Spoetl, C., Vennemann, T.W., 2003. Continuous-flow IRMS analysis of carbonate minerals. Rapid Commun. Mass Spectr. 17, 1004–1006.

Thompson, M.D., Bowring, S.A., 2000. Age of the Squantum 'tillite', Boston basin, Massachusetts: U–Pb zircon constraints on terminal Neoproterozoic glaciation. Am. J. Sci. 300, 630–655.

Vroon-ten Hove, M., 1997. A review of the Seismstratigraphy and play potential of the pre-salt Huqf in Oman. Petroleum Development Oman Exploration Report, 376.

Walter, M.R., Veevers, J.J., Calver, C.R., Gorjan, P., Hill, A.C., 2000. Dating the 840–544 Ma Neoproterozoic interval by isotopes of strontium, carbon, and sulfur in seawater, and some interpretative models. Precambrian Res. 100 (1–3), 371–433.

Wright, V.P., Ries, A.C., Munn, S.G., 1990. Intraplatformal basin-fill from the Infracambrian Huqf Group, east central Oman. In: Robertson, A.H.F., Searle, M.P., Ries, A.C. (Eds.), The Geology and Tectonics of the Oman Region. Geological Society Special Publication, pp. 601–616.

Xiao, S., et al., 2004. The Neoproterozoic Quruqtagh Group in eastern Chinese Tianshan: evidence for a post-Marinoan glaciation. Precambrian Res. 130 (1–4), 1–26.